

Chapter 2

Open-Circuit Fault Detection Methods for Three-Level Converters

2.1 Switch Fault Case and Reasons

IGBT modules are typically classified into two types: wire-bonded IGBT modules and press-pack IGBT modules. They have different characteristics which are a tradeoff between cost and performance, as shown in Table 2.1.

IGBT modules have a larger thermal resistance, a lower power density, and a higher failure rate because of the soldering and bond-wire connections of the internal chips. Press-pack packaging technology shown in Fig. 2.1 improves the connections between chips by direct press-pack contact. Therefore, press-pack IGBT modules have better reliability, a higher power density, and better cooling capability. However, their cost is also higher than that of conventional IGBT modules. Therefore, wire-bonded power device modules are still widely used in power electronics. Therefore, the failure mechanisms of conventional wire-bond IGBT modules are presented.

A wire-bonded IGBT is made up of several layers consisting of different materials. A silicon (Si) chip is soldered to a direct copper bonded (DCB) ceramic substrate. The DCB substrate insulates the Si chip from the baseplate and conducts the heat dissipated by the chip to the cooling system. Finally, the top side of the Si chip is contacted by aluminum (Al) bond wires. Figure 2.2 shows the structure of a wire-bond IGBT modules package.

The weak points in wire-bond IGBT modules are the wire bond and silicon interconnection, the silicon and DCB substrate solder joint, and the DCB substrate and baseplate solder joint. The primary failure mechanism in IGBT modules is the wire-bond liftoff as shown in Fig. 2.3. Al and Si material have different coefficients of thermal expansion (CTE), and thermal cycling causes repeated cooling and heating. This allows the disparately joined materials to expand and shrink at different rates when stress is applied at the point of contact. This CTE mismatch with temperature swings leads to wire-bond liftoff failures.

Another dominant failure mechanism is solder joint fatigue as shown in Fig. 2.4. Two solder joints are present in a standard IGBT module. They are between the Si

Table 2.1 Wire-bond IGBT modules versus press-pack IGBT modules

Characteristic	Wire-bond module	Press-pack IGBT module
Power density	Moderate	High
Reliability	Moderate	High
Cost	Moderate	High
Failure mode	Open circuit	Short circuit
Ease of maintenance	Better	Worse
Insulation of heat sink	Yes	No
Thermal resistance	Moderate	Small
Switching loss	Low	Low
Conduction loss	High	High



Fig. 2.1 Press-pack IGBT module

and the DCB and between the DCB and the baseplate. The CTE mismatch between the DCB substrate and the baseplate is higher than that between the DCB substrate and the Si. Therefore, the possibility of failure is higher in the solder joint between the DCB and the baseplate. This solder joint degradation increases the thermal resistance of the power device module. Therefore, the temperature in the module increases, which accelerates the lifting of the wire-bond.

The faults of IGBTs are classified into short-switch faults and open-switch faults. Short-switch faults may have serious impact on systems such as breakdown, as shown in Fig. 2.5, because a large current (which is above the rated current) flows through the short-circuited switch. Therefore, the system has to stop to ensure the safety of the other parts and the fuse, or additional devices, as shown in Fig. 2.6 [2], are used for preventing explosion from an abnormal large current.

On the other hand, open-switch faults (which are generated by thermal cycling, excessive collector current, and gate driver faults) cause input current distortions in NPC and T-type three-level converters [9, 10]. For the input side of the rectifier, this current distortion increases the total harmonic distortion (THD) and adversely affects the grid. Moreover, the power factor of the rectifier decreases, and the DC-link ripple increases. If an open-switch fault is not detected for a long time, other problems are generated because the distorted current is used to control the

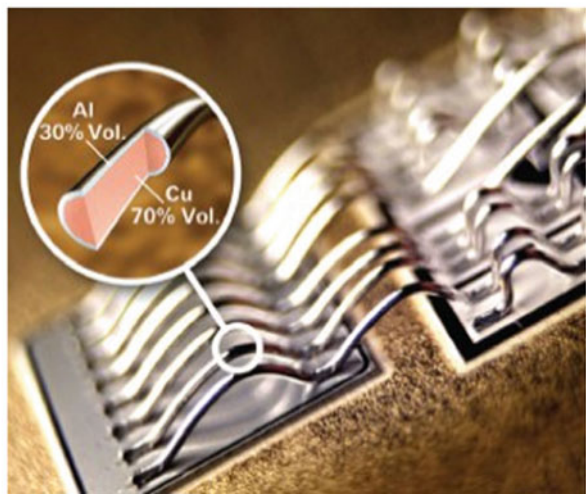
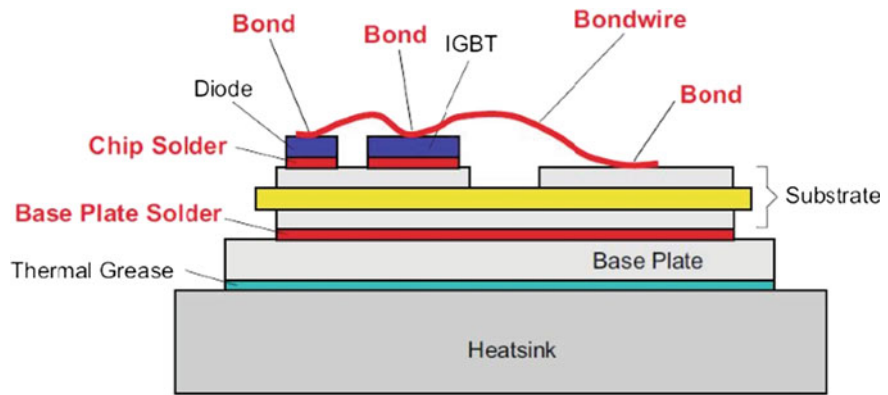


Fig. 2.2 Wire-bond IGBT module

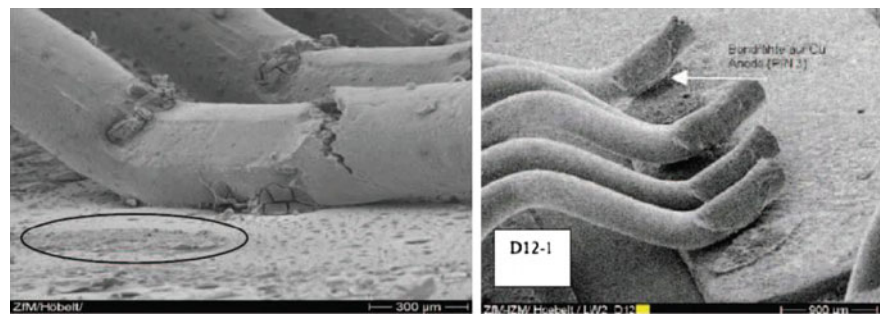


Fig. 2.3 Fault cases of a wire-bond IGBT module (wire fatigue)

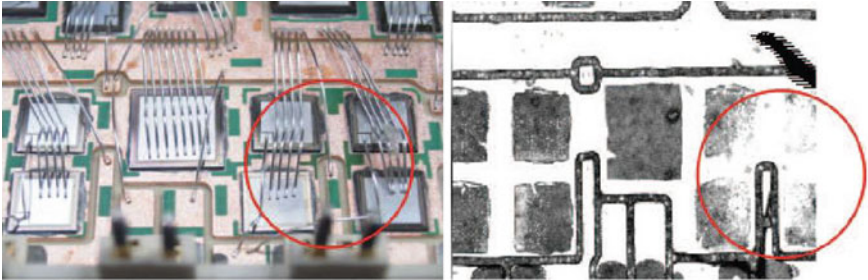


Fig. 2.4 Fault cases of a wire-bond IGBT module (solder fatigue)

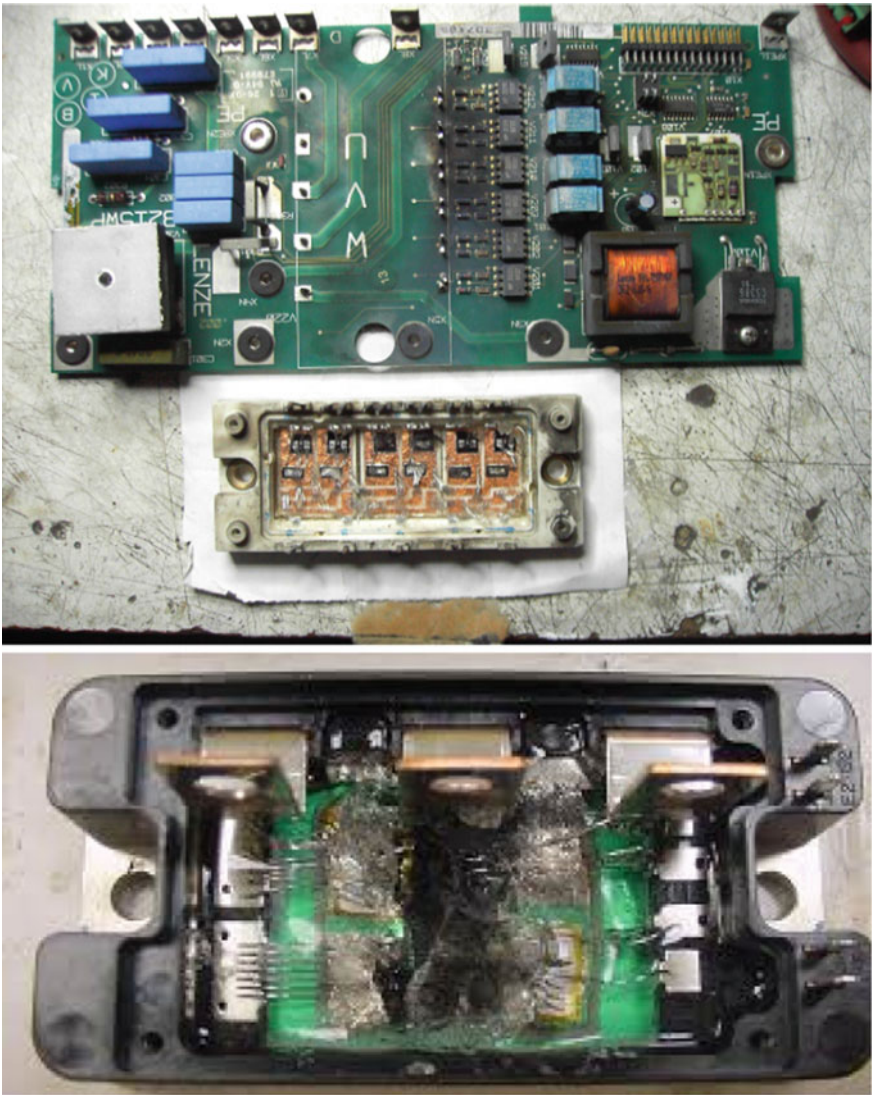


Fig. 2.5 Breakdown case

characteristic according to the operation mode (inverter mode and rectifier mode) will be explained. Finally, based on these results, several detection methods will be demonstrated.

2.2 Switch Open-Circuit Fault Detection Methods for NPC Three-Level Inverters

The three-level converter is used as a power conversion system in motor drives and renewable energy generation. Inverter operation means that the energy stored in the DC-link is transferred to the output of the inverter. This chapter shows switch open-circuit fault detection methods for NPC three-level inverters.

2.2.1 Switch Open-Circuit Fault Detection Methods Using Additional Devices

A. Switch open-circuit fault detection method using voltage sensors

Figure 2.7 shows a two-level inverter used in motor drive applications [1]. There are voltage sensors for detecting switch open-circuit faults. This method uses the fact that the output voltage of the three legs cannot make the desired output voltage

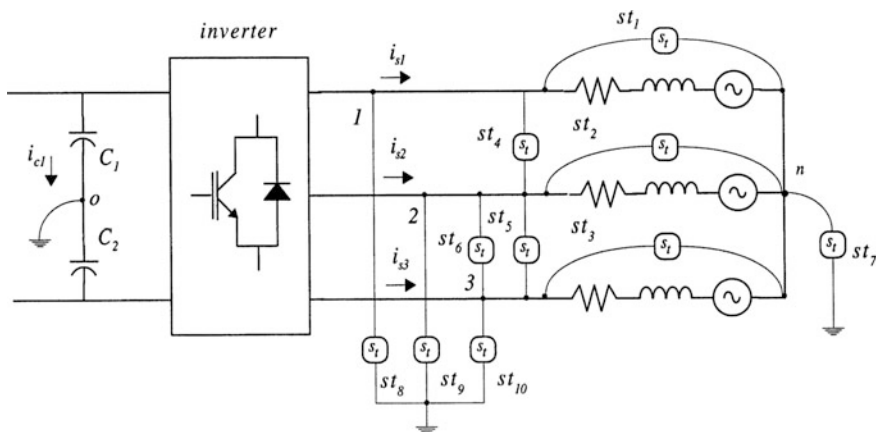


Fig. 2.7 Switch open-circuit fault detection method using voltage sensors (reprinted from Ref. [1], Fig. 4)

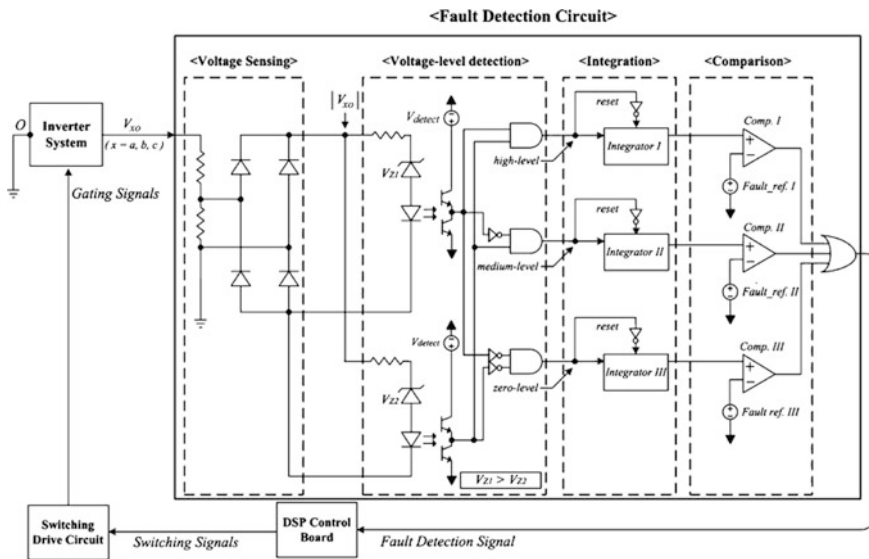


Fig. 2.8 Switch open-circuit fault detection method using additional detection circuits (reprinted from [3], Fig. 9)

in the presence of a switch open-circuit fault. In this method, the detection signal is generated by comparing two voltages in the normal condition and in the switch fault condition.

B. Switch open-circuit fault detection method using additional detection circuits

Figure 2.8 shows a detection circuits for switch open-circuit faults [3]. The inputs of the detection circuits are the pole voltage (V_{x0} , $x = a, b, c$) of each leg and the fault signal is generated through the Voltage-level detection circuit, the Integration circuit, and the Comparison circuit in order. This method can identify a fault state exactly. However, it cannot distinguish the position of the switch fault.

2.2.2 Switch Open-Circuit Fault Detection Method Using Current Distortion

The detection methods using additional devices have big drawbacks due to their increases in terms of size and cost. Therefore, a lot of papers have proposed detection methods using current distortion without additional devices.

The abnormal voltage caused by a switch open-circuit fault leads to current distortion. The output currents which are measured by current sensors are used to control the system and to obtain useful information for detecting fault switches.

A. The effects on current from switch open-circuit faults

The basic operation of a NPC three-level converter is shown in Chap. 1. The switching states are divided into three states P, O, and N. By considering the current direction, six current paths are expressed as shown in Fig. 2.9. When the switching state is P, there are two current paths depending on the current direction. In one path, the current flows through the two switches and the current direction is from the output to the DC-link. In the other path, the current direction is from the

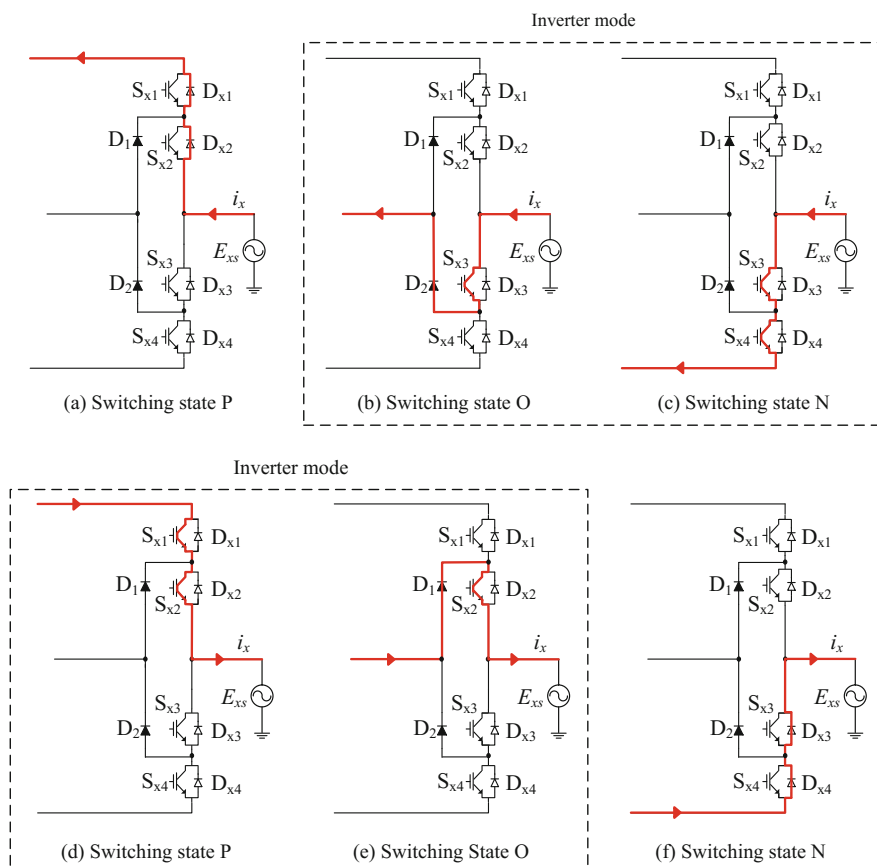


Fig. 2.9 Current paths of the NPC topology for the current directions and switching states

DC-link to the output and the current flows through two diodes. Based on the results, the switching states O and N can be analyzed.

When the NPC three-level converter operates in the inverter mode with unity power factor, only four current paths are used because the sign of the output voltage is the same as that of the output current. A positive output voltage is generated by the P- and O-switching states and the current flows from the DC-link to the output. The N- and O-switching states lead to a negative output voltage and the current flows from the output to the DC-link. The P- (or N-) switching state is a valid switching state which causes the current to flow in the inverter mode. The O-switching state act as a freewheeling path.

- S_{x1} open-circuit fault

When the open-switch fault occurs in switch S_{x1} while the switching state is “P,” the phase current path in the grid-connected system is different from that under the RL load condition. Because of the grid phase voltage E_{xs} , the diode D_1 becomes reverse-biased. The grid phase voltage E_{xs} is the voltage between the grid and ground. The current path is opened, and the positive phase current becomes zero as shown in Fig. 2.10a. If E_{xs} is higher than the dc-link voltage ($V_{DC}/2$), the current path is formed through diodes D_{x1} and D_{x2} . Since this period is very short and the potential difference is very small, the negative phase current is almost zero.

- S_{x2} open-circuit fault

When the open-switch fault occurs in switch S_{x2} while the switching state is “P,” the phase current does not flow as shown in Fig. 2.10b, because the phase current path is opened. Even when the switching state is “O,” the phase current path is not formed, because the switch S_{x2} is opened. If E_{xs} is higher than V_{xz} , the phase current is formed through switch S_{x3} and diode D_2 . However, the negative phase current does not flow, because this period is very short.

- S_{x3} open-circuit fault

When the switching state is “N,” the phase current path is opened because of the occurrence of the open-switch fault in switch S_{x3} . The negative phase current becomes zero as shown in Fig. 2.10c.

Even when the switching state is “O,” the phase current path is not formed, because switch S_{x3} is opened. The path is formed through diode D_1 and switch S_{x2} when V_{xz} is higher than E_{xs} . However, the positive phase current does not flow because of the abovementioned reasons.

Table 2.2 Feasible and infeasible switching state of a T-type three-level converter depending on the position of the open-switch fault

Position of open-switch fault	Feasible switching state	Infeasible switching state
S_{x1}	N (Fig. 2.9c, f) O (Fig. 2.9b, e) P (Fig. 2.9a)	P (Fig. 2.9d)
S_{x2}	N (Fig. 2.9c, f) O (Fig. 2.9b) P (Fig. 2.9a)	P (Fig. 2.9d) O (Fig. 2.9e)
S_{x3}	N (Fig. 2.9f) O (Fig. 2.9e) P (Fig. 2.9a, d)	N (Fig. 2.9c) O (Fig. 2.9b)
S_{x4}	N (Fig. 2.9f) O (Fig. 2.9b, e) P (Fig. 2.9a, d)	N (Fig. 2.9c)

- S_{x4} open-circuit fault

When the open-switch fault occurs in switch S_{x4} while the switching state is “N,” diode D_2 becomes reverse biased. The current path follows the open circuit, and the phase current becomes zero as shown in Fig. 2.10d.

The feasible and infeasible switching states of NPC three-level converter depending on the position of the open-switch fault are summarized in Table 2.2.

B. Analysis of the current distortion caused by open-circuit faults

The measured three-phase currents (I_a , I_b , I_c) can be transformed into two dimensions (I_{ds} , I_{qs}) through the following equations:

$$\begin{aligned} I_{ds} &= I_a \\ I_{qs} &= \frac{1}{\sqrt{3}}(I_b - I_c) \end{aligned} \quad (2.1)$$

The current patterns that indicate the location of a faulty switch can be classified into 12 patterns. The shape of the current pattern under a healthy condition is a circle [4, 5].

In the occurrence of an open-switch fault, there is a change in the phase current value at the location where the fault has occurred. Therefore, a change in the circle shape and angle represents the occurrence of an open fault condition and is an indicator of the location of the faulty switching device, as shown in Table 2.3 and Fig. 2.11 under RL load. The magnitude and semicircle angle are defined as:

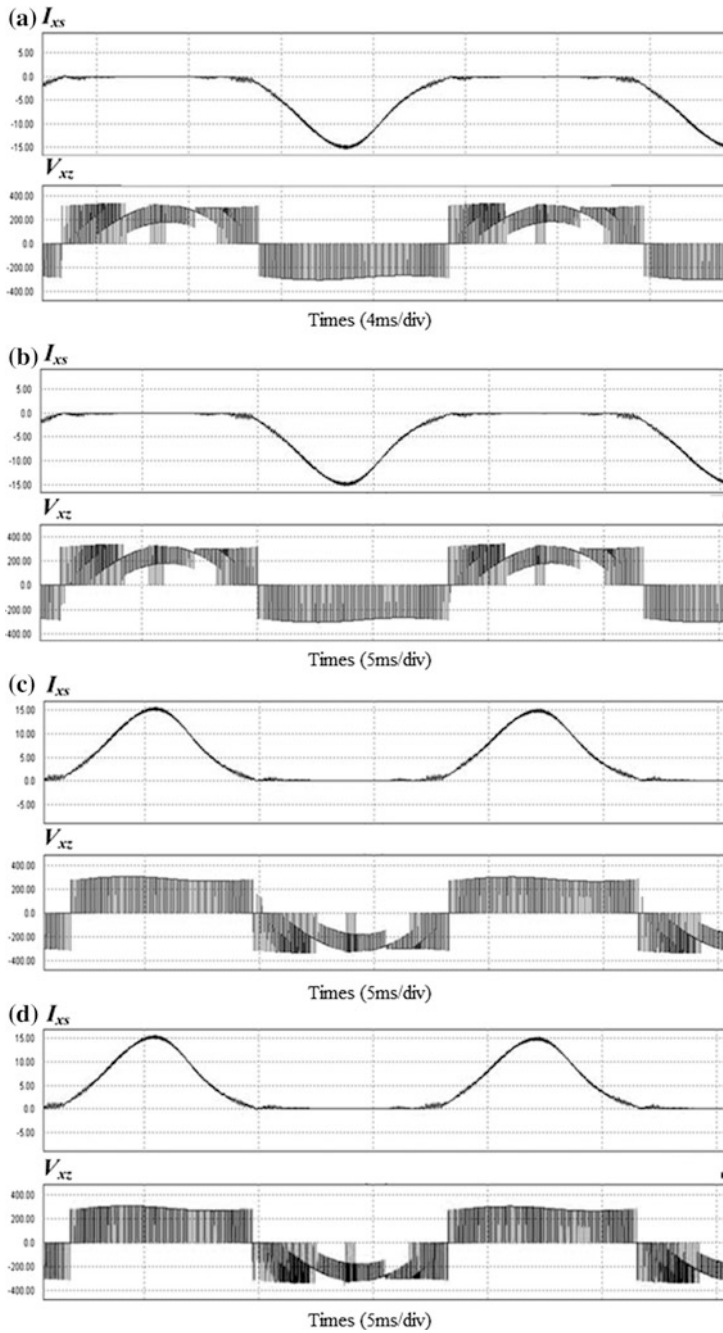


Fig. 2.10 Grid-connected NPC inverter characteristics: **a** S_{x1} , **b** S_{x2} , **c** S_{x3} , **d** S_{x4} (reprinted from [4], Figs. 10–13)

Table 2.3 Angle of semicircles during the occurrence of an open-switch fault

θ	Fault switch
$30^\circ\text{--}90^\circ$	S_{c1} or S_{c2} fault
$90^\circ\text{--}150^\circ$	S_{b3} or S_{b4} fault
$150^\circ\text{--}210^\circ$	S_{a1} or S_{a2} fault
$210^\circ\text{--}270^\circ$	S_{c3} or S_{c4} fault
$270^\circ\text{--}330^\circ$	S_{b1} or S_{b2} fault
$330^\circ\text{--}30^\circ$	S_{a3} or S_{a4} fault

$$I_{mag} = \sqrt{I_{qs}^2 + I_{ds}^2} \quad (2.2)$$

$$\theta = \tan^{-1} \left(\frac{I_{qs}}{I_{ds}} \right) \quad (2.3)$$

The open-switch fault detection steps under RL load are as follows

- (1) First, calculate the magnitude of the current vector using (2.2).
- (2) Second, compare I_{mag} with the magnitude of the current reference.

$$I_{mag,ref} = \sqrt{I_{qe,ref}^2 + I_{de,ref}^2} \quad (2.4)$$

- (3) Third, if the difference of (2.2) exceeds the defined value, determine the angle of (2.3).
- (4) Fourth, determine the position of the open-circuit fault by Table 2.3.

In the third step, by dividing the detection level into two levels, S_{x1} and S_{x2} (or S_{x3} and S_{x4}) the faults can be classified.

Figure 2.12 shows the current patterns of a grid-connected NPC inverter system under the fault condition. As in the previous analysis, the phase currents are the same in the two situations when either the S_{x1} switch or the S_{x2} switch are broken down. The phase currents when a fault occurs in either S_{x3} or S_{x4} are also equal. It is impossible to distinguish a fault in switch S_{x1} from that in switch S_{x2} , or a fault in switch S_{x3} from that in switch S_{x4} using the method explained in the previous section.

C. Experimental result of switch open-circuit fault detection in NPC three-level inverters

- S_{x1} and S_{x2} (S_{x3} and S_{x4}) classification using the pulse of the O-switching state

The main difference between a fault in switch S_{x1} and that in switch S_{x2} or between a fault in switch S_{x3} and that in switch S_{x4} is the possibility of switching state O. However, E_{xs} nullifies positive phase current and negative phase current,

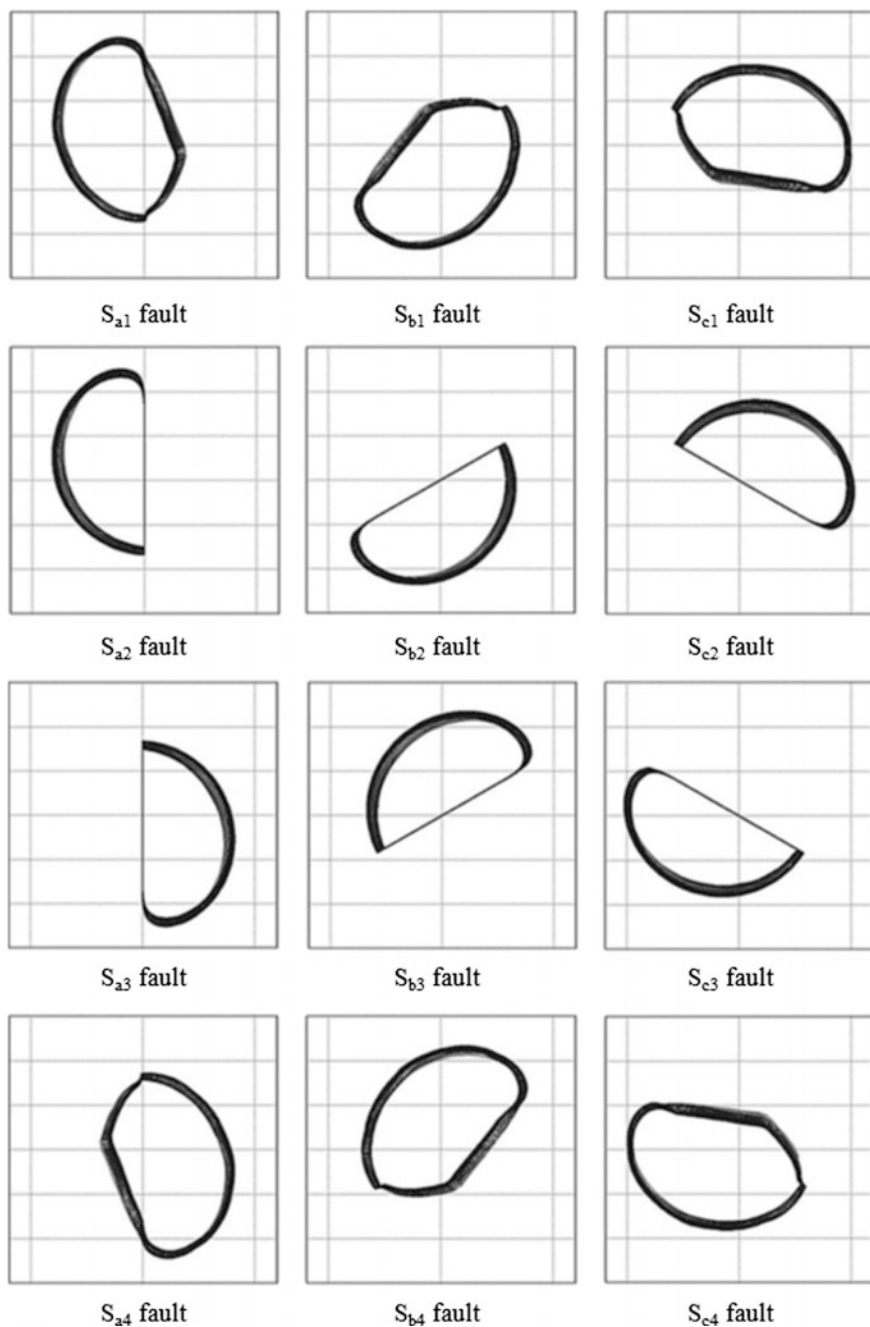


Fig. 2.11 Simulated current patterns during the occurrence of an open-switch fault under RL load (reprinted from [4], Fig. 9)

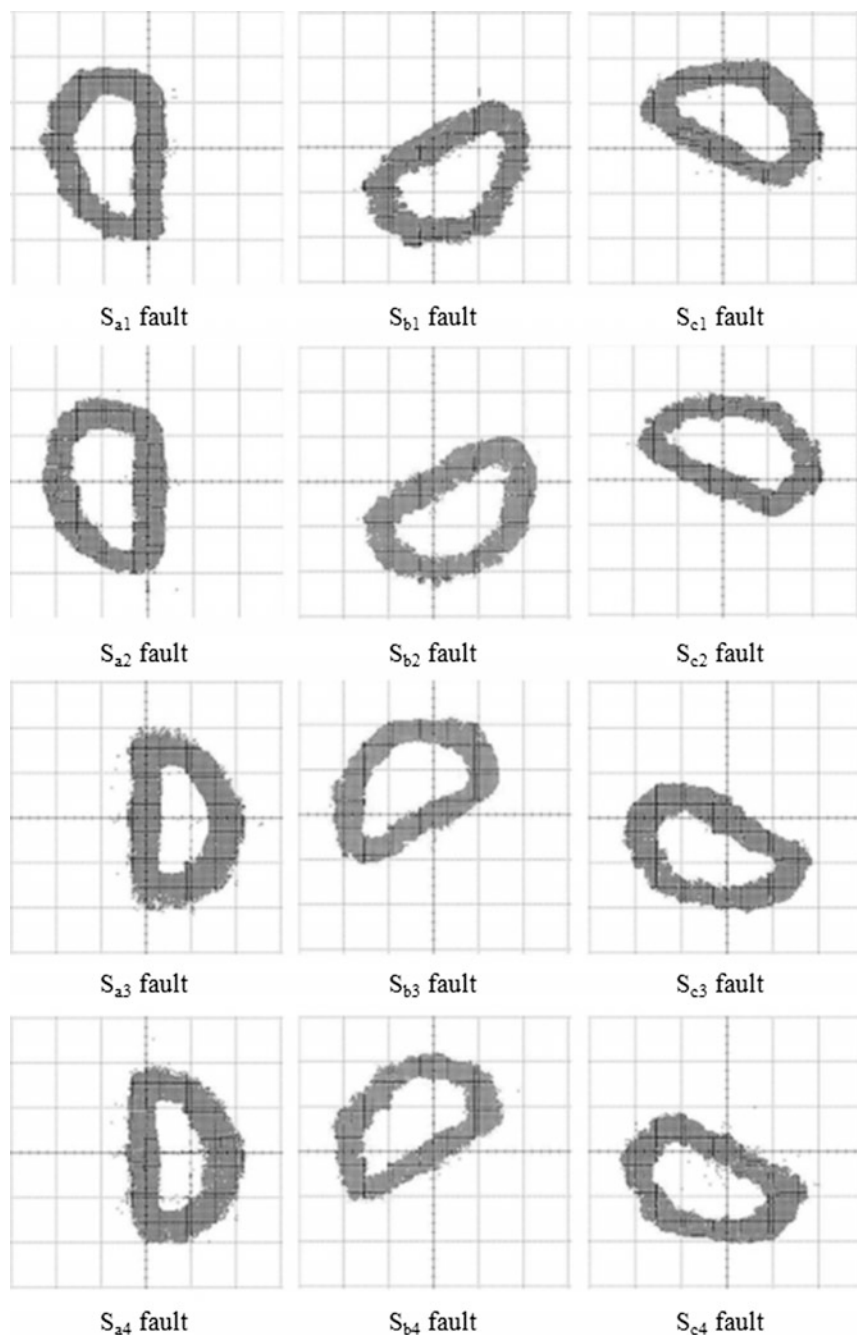


Fig. 2.12 Measured current patterns during the occurrence of an open-switch fault in a grid-connected system (reprinted from [4], Fig. 30)

regardless of the possibility of the O-switching state. It is difficult to determine the effects of the O-switching state on the current patterns. It is only possible to determine whether an open-switch fault occurs in one of the two upper switches (S_{x1} , S_{x2}) or in one of the two lower switches (S_{x3} , S_{x4}), on the basis of the current patterns. The location of a faulty switch either between the two upper switches or between the two lower switches in a grid-connected NPC inverter system can be identified by adding a simple switching scheme to the conventional method.

(5.1) Current generation identification using the pulse of the O-switching state [4]

If an open-switch fault occurs in one of the two upper switches, the O-switching state is applied for a very short period when E_{xs} is negative. If positive phase current flows for a short period, then it can be inferred that an open-switch fault has occurred in switch S_{x1} . If positive current does not flow, then it can be inferred that an open-switch fault has occurred in switch S_{x2} .

If an open-switch fault occurs in one of the two lower switches, the O-switching state is applied for a very short period when E_{xs} is positive. If negative phase current flows for a short period, then it can be inferred that an open-switch fault has occurred in switch S_{x4} . If negative current does not flow, it can be inferred that an open-switch fault has occurred in switch S_{x3} .

Figure 2.13a shows experimental results under the parameters of Table 2.4 when an open-switch fault occurs in switch S_{x1} . It is possible to detect the open-switch fault within half of a fundamental period and to identify the location of the faulty switch within two fundamental periods. Figure 2.13b shows the fault signal, phase angle, and phase current when an open-switch fault occurs in switch S_{x2} . Similarly, Fig. 2.13c, d show the phase angle, fault signal, and phase current when an open-switch fault occurs in switches S_{x3} and S_{x4} , respectively. Open switch fault detection is also possible within half of a fundamental period, and identification of the faulty switch is possible within two fundamental periods. It is noted here that a satisfactory diagnosis is obtained. It can also be seen from the experimental results that the location of the faulty switch can be identified with the proposed algorithm by using a simple switching control.

- S_{x1} and S_{x2} (S_{x3} and S_{x4}) classification using reactive current injection [11]

Usually, grid-connected inverters transfer electric power to the grid with a unity Power Factor (PF). Therefore, the polarities of the output phase current and the output voltage are almost the same, as shown in Fig. 2.14a. If an under excited reactive power is injected, the phase current leads the output pole voltage and grid voltage. Therefore, regions that have the different polarities between the phase

Table 2.4 Experimental parameters

DC-link voltage	600 V	Line-to-line voltage	380 Vrms
DC-link capacitor	1230 μ F	Control period	160 μ s
Switching frequency	6.25 kHz	Injection time for the O switching state	1–2 ms

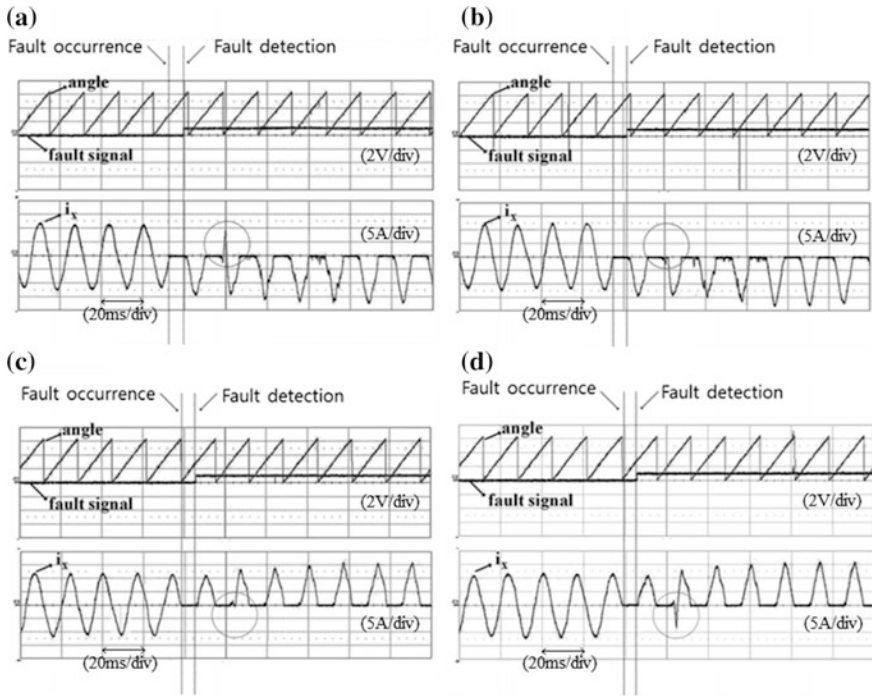


Fig. 2.13 Measured results of fault diagnosis when an open-switch fault occurs: **a** S_{a1} , **b** S_{a2} , **c** S_{a3} , **d** S_{a4} (reprinted from Ref. [4], Figs. 31–34)

current and the output voltage occur as shown in Fig. 2.14b. In this section, region 1 means that the phase current is positive and that the output pole voltage is negative, while region 2 means that the phase current is negative and that the output voltage is positive. By making regions 1 and 2 through under excited reactive power injection, the possibility of O-switching state can be determined and the faulty switch can be identified. Whether or not the current in regions 1 or 2 flows depending on the faulty switch.

(5.2) Current generation identification using reactive current injection [11]

First detection steps 1–4 are performed. Then reactive current is injected. If current is generated, the fault switch is S_{x4} (or S_{x1}), if it is not generated, the switch is S_{x2} (or S_{x3}).

Figure 2.15 shows experimental results under the parameters of Table 2.5. In the case of a S_{a1} fault, positive phase current flows in the region where under excited current is injected as shown in Fig. 2.15a. However, if an open-circuit fault occurs in S_{a2} , positive current does not flow as shown in Fig. 2.15b. From this result, the

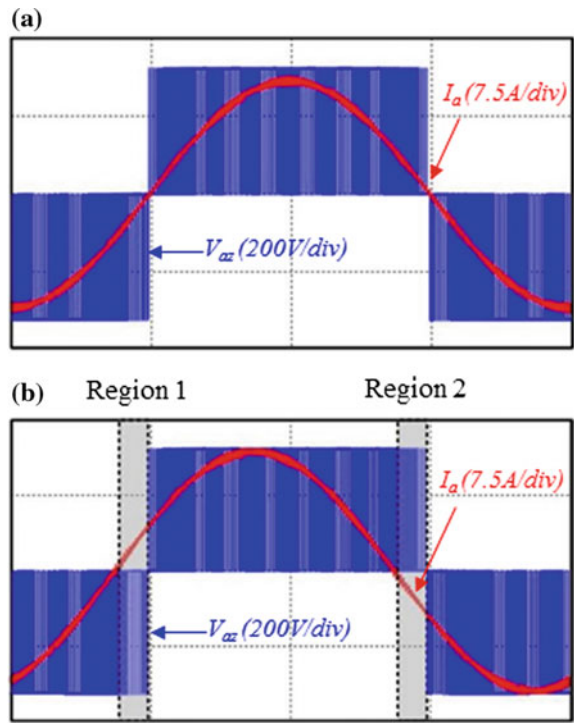


Fig. 2.14 Phase currents I_a and pole voltage V_{az} : **a** before and **b** after the injection of under excited reactive current (reprinted from [11], Fig. 6)

Table 2.5 Experiment parameters

DC-link voltage	600 V	Line-to-line voltage	380 Vrms
DC-link capacitor	2200 μ F	Control period	100 μ s
Switching frequency	10 kHz	Injection time for O switching state	2 A

faulty switch between the upper two switches can be correctly identified. Figure 2.15c, d show experimental results obtained with the discussed fault detection method when Type-A open-circuit faults have occurred in S_{a3} and S_{a4} , respectively. To determine the fault location from between the two lower switches (S_{a3} and S_{a4}), under excited reactive current has been injected. Negative current does not flow under an open-circuit fault in S_{a3} . However, negative current flows in the case of an open-circuit fault in S_{a4} . The location of the faulty switch is identified precisely by the discussed method.

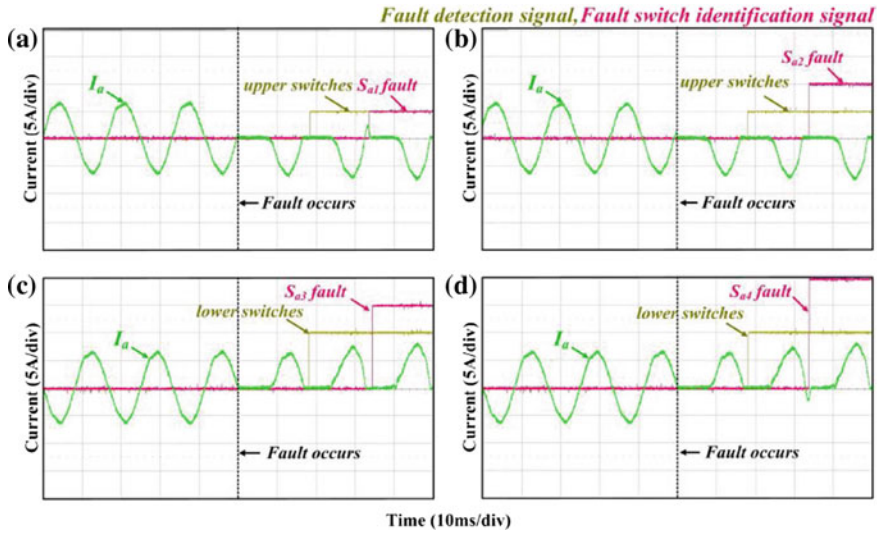


Fig. 2.15 Diagnosis of a faulty switch under a type-A open-circuit fault in: **a** S_{a1} , **b** S_{a2} , **c** S_{a3} , **d** S_{a4} by the injection of under excited reactive current (reprinted from [11], Fig. 20)

2.3 Switch Open-Circuit Fault Detection Methods for NPC Three-Level Rectifiers

2.3.1 Switch Open-Circuit Fault Detection Method Using Additional Devices

Switch open-circuit fault detection methods using additional devices can detect the position of an open-circuit fault regardless of the operation mode (inverter mode or rectifier mode). The methods mentioned in Sect. 2.2.1 can be used for detecting switch faults in NPC-type three-level rectifiers.

2.3.2 Switch Open-Circuit Fault Detection Method Using Current Distortion

A. The effects on current from switch open-circuit faults

The operating status of the switches and the pole voltage in NPC inverters can be represented by switching states. The switching state P indicates that the two upper switches S_{x1} and S_{x2} are ON and that the pole voltage V_{xz} , which is the voltage at terminal x ($x = a, b, c$) with respect to the neutral-point voltage Z , is $+V_{dc}/2$. The

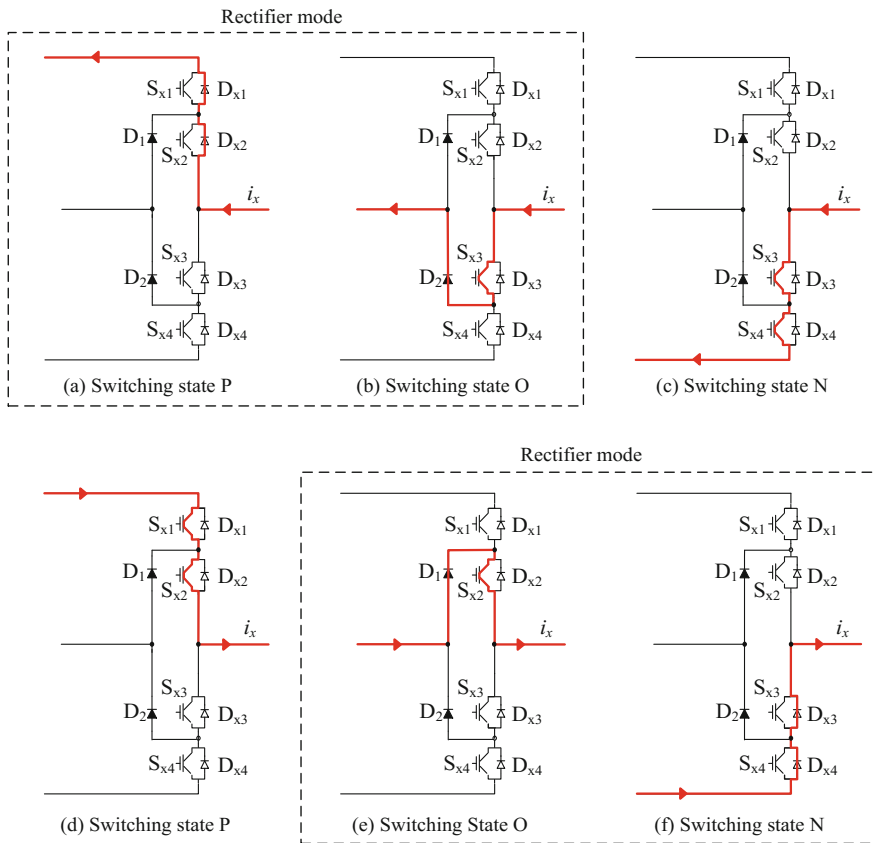


Fig. 2.16 Current paths of the NPC topology for the current directions and switching states

switching state O denotes that the two inner switches S_{x2} and S_{x3} are ON and that V_{xz} is zero. The switching state N signifies that the two lower switches S_{x3} and S_{x4} are ON and that $V_{xz} = -V_{dc}/2$.

Figure 2.16 shows the current paths according to the switching state and the phase current direction. The phase current includes information on the switching states in the NPC inverter. If an open-switch fault occurs, the switching state does not reach the desired state. This causes a change in V_{xz} and the phase current i_x .

B. S_{x1} and S_{x4} open-circuit faults of the three-level converters used in WTSs [8, 12]

Figure 2.17 shows a back-to-back power converter using a neutral-point-clamped (NPC) topology in a Wind Turbine Systems (WTS). The voltage difference ΔV between the input voltage, provided by the NPC rectifier, and the back electromotive force (EMF) of the PMSG generates input current, which has a different phase angle than the voltage difference ΔV because of the inductance and resistance of the PMSG. The magnitude of the input voltage is almost the same as

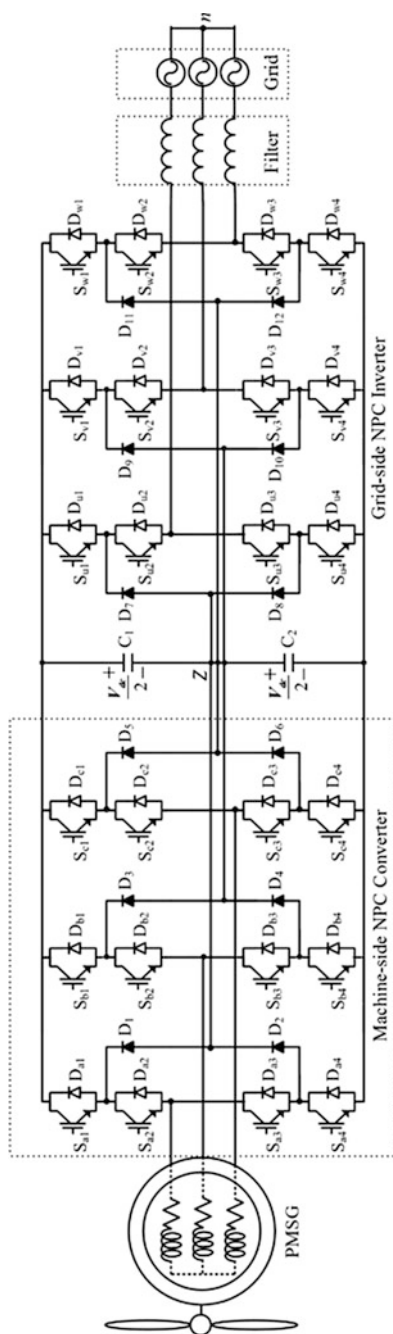


Fig. 2.17 Back-to-back converter using the NPC topology for a WTS (reprinted from [8], Fig. 1)

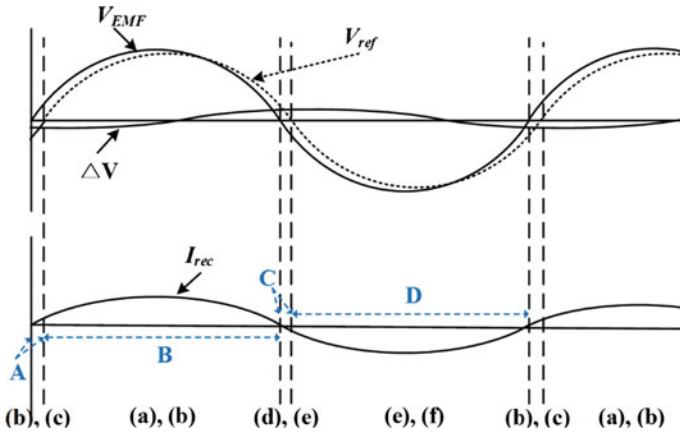


Fig. 2.18 Normal current flow between a NPC rectifier and a PMSG (reprinted from [12], Fig. 4)

(or smaller than) the back EMF. If the two voltage magnitudes are almost the same, the current magnitude is determined by the phase angle difference between the input voltage and the back EMF. Zero current means that the two voltages are the same and that the phase angle of the input voltage matches that of the back EMF. For unity power factor, the input voltage is controlled to correspond to the phase of the current with the same phase as the back EMF, as shown in Fig. 2.18.

If the time intervals containing the paths in Fig. 2.16c, d are not long enough to distort the current, S_{x2} and S_{x3} open-switch faults (which are related to the paths of Fig. 2.16b, e, excluding S_{x1} and S_{x4} open-switch faults) can be considered because there is no current through the IGBTs in the paths of Fig. 2.16a, f. Therefore, the switching state O, which is shown in Fig. 2.16b, e, is a valid switching state that generates current in the rectifier.

However, the time intervals of [(b), (c)] and [(d), (e)] are influenced by the current magnitude and modulation index. There are two Cases causing wide intervals [(b), (c)] and [(d), (e)]:

- Case 1: When V_{EMF} is small and a large I_{rec} is required
- Case 2: When reactive current is injected for the IPMSG

Figure 2.19 shows the current flow when a NPC rectifier generates a large current with a small modulation index. To create a large current flow, the phase angle difference is expanded. As a result, the time intervals of [(b), (c)] and [(d), (e)] increase. In this case, current distortion is generated by S_{x1} and S_{x4} open-switch faults. Consequently, all of the open-switch faults in the rectifier must be considered.

C. Open-circuit faults detection of the three-level converters used in WTSs

The current pattern is divided into four patterns depending on the location of the open-switch fault. An S_{x2} open-switch fault prevents the generation of negative

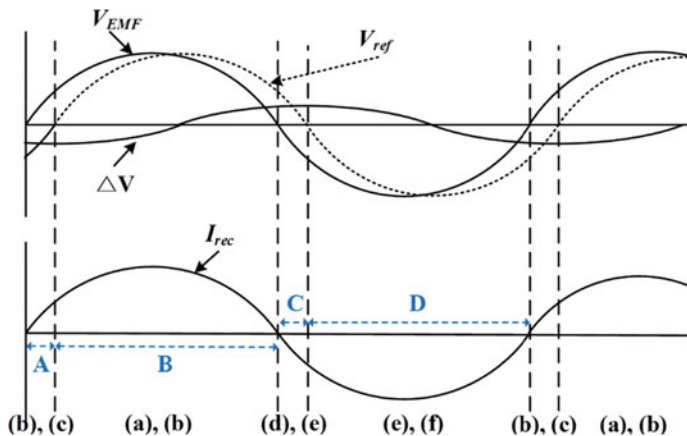


Fig. 2.19 Current flow process with a small modulation index and a large current (reprinted from [12], Fig. 5)

current, and an S_{x3} open-switch fault prevents the generation of positive current. An S_{x1} open-switch fault makes the current zero for some duration in the negative current, while the current becomes zero for some duration in the positive current when an S_{x4} open-switch fault occurs.

The range where the current distortion occurs can be defined as shown in Fig. 2.20. In each range, a switch open-circuit fault makes the current zero.

In the discussed detection method, the current can be divided into three ranges, as shown in Fig. 2.21, to separate the four patterns. The time of the zero range $T_{Z,Lx}$ is used to detect the location of an open-switch fault. The current belongs in one of the three ranges. If an S_{x2} open-switch fault occurs, no current flows in the negative range. An S_{x3} open-switch fault prevents current from flowing in the positive range, and the current is in the zero range for a longer time.

If the previous sign of the current was positive and if the current is in the zero range for half of a period, this indicates an S_{x2} open-switch fault, as shown in Fig. 2.21c. In the case of an S_{x3} open-switch fault, the previous sign of the input current is negative, and all of the other characteristics are the same as those in the S_{x2} open-switch fault detection method.

The detection method for the $T_{Z,Lx}$ of S_{x2} and S_{x3} open-switch faults is expressed as:

$$D_{23} = R_{23} T_{half} = R_{23} \frac{1}{2f_s} < T_Z \quad \begin{cases} \text{if } C_{pre,sign} = \text{Positive}, S_{x2} \text{ fault} \\ \text{if } C_{pre,sign} = \text{Negative}, S_{x3} \text{ fault} \end{cases} \quad (2.5)$$

where R_{23} is the detection parameter, $C_{pre,sign,Lx}$ is the previous sign of the current, T_{half} is half of the current period, and f_s is the angular frequency of the PMSG.

The previous sign of the current is determined when the input current enters the zero range and the time of the zero range is calculated, as shown in Fig. 2.22.

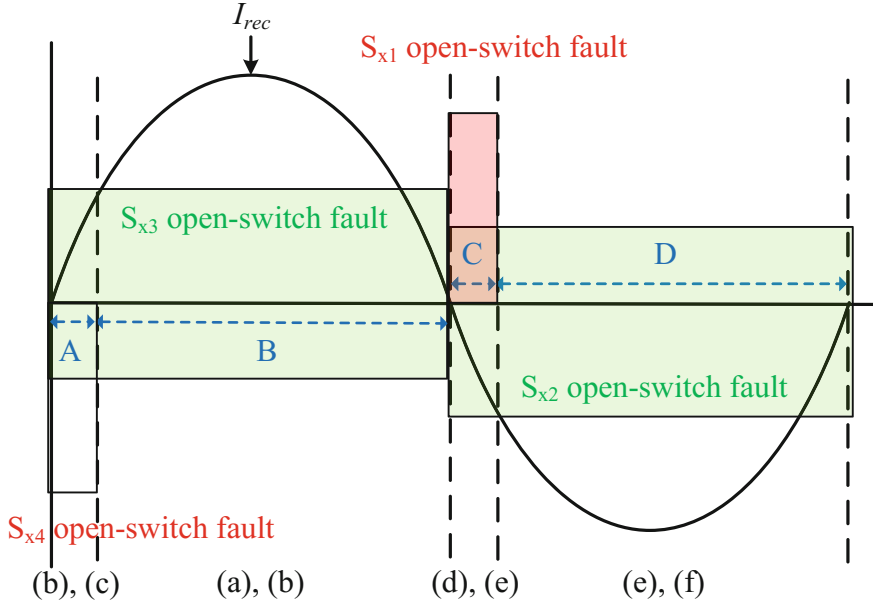


Fig. 2.20 Current distortion range depending on the position of a switch open-circuit fault (reprinted from [12], Fig. 6)

S_{x1} and S_{x4} open-switch faults are also detected by calculating $T_{Z,IX}$. When the current is sinusoidal, T_P and T_N are almost the same, and $T_{Z,IX}$ is small. However, an S_{x1} open-switch fault leads to a decrease in T_N and an increase in $T_{Z,IX}$, as shown in Fig. 2.21b, and an S_{x4} open-switch fault decreases T_P and increases $T_{Z,IX}$. Therefore, the detection method for S_{x1} and S_{x4} open-switch faults is expressed as:

$$D_{14} = R_{14} T_{half} = R_{14} \frac{1}{2f_s} < T_Z \quad \begin{cases} \text{if } C_{pre,sign} = \text{Positive}, S_{x1} \text{ fault} \\ \text{if } C_{pre,sign} = \text{Negative}, S_{x4} \text{ fault} \end{cases} \quad (2.6)$$

where R_{14} is the detection parameter.

To determine the zero range value, the current ripple is considered. 10% of the current is used in this study. T_{half} for open-switch fault detection is changed depending on the angular frequency because the period of the current is proportional to the speed of the PMSG.

- Determination of the R_{23} and R_{14} values

In the determination of the R_{23} and R_{14} values, the zero range value due to each open-switch fault should be considered. When an S_{x2} or S_{x3} open-switch fault occurs, $T_{Z,IX}$ is almost the same as a half period of f_s ($1/2 f_s$) regardless of the system parameters. Therefore, if R_{23} is lower than 1, it is possible to detect S_{x2} and S_{x3}

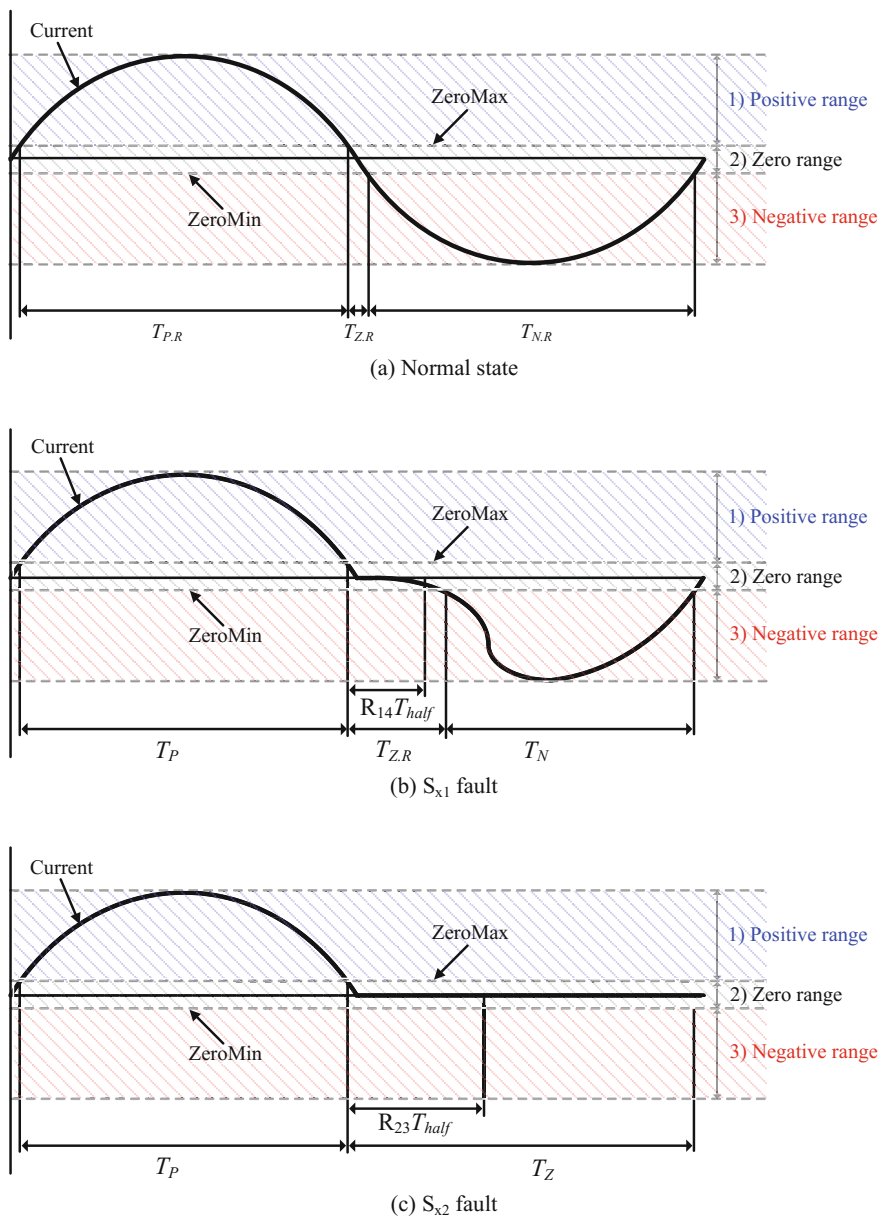


Fig. 2.21 Concept of the open switch fault detection method (reprinted from [8], Figs. 9, 10, 12)

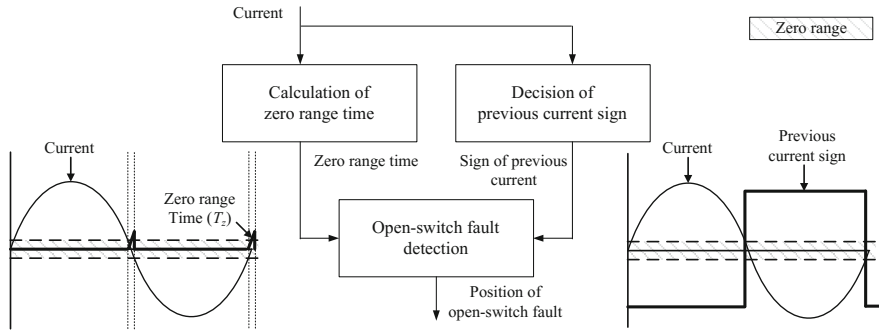


Fig. 2.22 Block diagram for the detection of the previous current sign and the calculation of the zero range duration (reprinted from Ref. [8], Fig. 11)

open-switch faults, and the detection performance can be improved by decreasing R_{23} close to 0.

To selecting R_{14} , the zero range value $T_{Z,IX}$ caused by an S_{x1} or S_{x4} open-switch fault should be considered. Regardless of the open-switch fault, 10% of the current is contained in the zero range, and its range θ_n is expressed as:

$$\theta_n = 2 \times \sin^{-1} \left(\frac{1}{10} \right) = 11.5^\circ \quad (2.7)$$

To consider the time of the zero range $T_{Z,IX}$ caused by an S_{x1} or S_{x4} open-switch fault, the system parameters shown in Fig. 2.23 are used. The voltage–current equation is expressed as

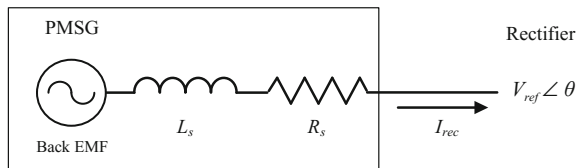
$$I_{x,rec} = \frac{BackEMF - V_{ref} \angle \theta}{R_s + j2\pi f_s L_s} \quad (2.8)$$

where V_{ref} is the rectifier input voltage and θ is the phase angle difference between the input voltage and the Back EMF.

θ is represented as:

$$\theta = \frac{-I_{x,rec} \times 2\pi f_s L_s}{BackEMF - I_{x,rec} R_s} \frac{360^\circ}{\pi} \quad (2.9)$$

Fig. 2.23 PMSG circuit model (reprinted from [8], Fig. 13)



When an S_{x1} or S_{x4} open-switch fault occurs, the range of the zero current θ_{fault} is expressed as:

$$\theta_{fault} = \theta + \frac{\theta_n}{2} \quad (2.10)$$

For selecting R_{14} , the requirement can be expressed as:

$$\frac{\theta_n}{180^\circ} \frac{1}{2f_s} < R_{14} \frac{1}{2f_s} < \frac{\theta_{fault}}{180^\circ} \frac{1}{2f_s} \quad (2.11)$$

Consequently, the values of R_{23} and R_{14} are in the range of 0–1, and R_{23} should be larger than R_{14} because the $T_{Z,Lx}$ for S_{x2} and S_{x3} open-switch faults is longer than that for S_{x1} and S_{x4} open-switch faults. R_{14} should satisfy (2.11).

The location of an open-switch fault in a rectifier can be detected using (2.5) and (2.6). S_{x2} and S_{x3} open-switch faults satisfy both (2.5) and (2.6). However, S_{x1} and S_{x4} open-switch faults satisfy only (2.6). Therefore, an open-switch fault is detected using (2.6). Then (2.6) is used to determine the location of the open-switch fault. The proposed detection method is applied to three-phase currents.

- Detection principle for open-switch faults in NPC inverters

There are two current patterns caused by open-switch faults in an inverter with a unity power factor. These are the same as those in the cases of S_{x2} and S_{x3} open-switch faults in a rectifier. In the non-unity power factor case, although S_{x1} and S_{x2} open-switch faults create different current patterns, these faults generate the same pattern for at least one-quarter of a period of the current (from the starting point of the zero current), as shown in Fig. 2.24.

Therefore, (2.6) can be used to detect an open-switch faults in an inverter. The previous sign of the current and the duration of the zero range are determined in the same procedure of the rectifier, as shown in Fig. 2.22. The detection equation for open-switch faults of an inverter is expressed as:

$$D_{up,low} = I_{up,low} T_{half} = I_{up,low} \frac{1}{2 \times 60} > T_{Z,Lx} \quad (2.12)$$

$$\begin{cases} \text{if } C_{pre,sign,Lx} = \text{Positive}, S_{x1} \text{ fault or } S_{x2} \text{ fault} \\ \text{if } C_{pre,sign,Lx} = \text{Negative}, S_{x3} \text{ fault or } S_{x4} \text{ fault} \end{cases}$$

where $I_{up,low}$ is the detection parameter. A grid frequency of 60 Hz is used for f_s , and $I_{up,low}$ should be in the range of 0–0.5 due to the zero power factor.

The location of an open-switch fault can be classified into an upper-side (S_{x1} and S_{x2}) fault or a lower-side (S_{x3} and S_{x4}) fault using this detection method. When the open-switch fault detection method using the duration of the zero current is applied to a back-to-back converter using the NPC topology, a block diagram of the open-switch fault detection method for the back-to-back converter is shown in Fig. 2.25.

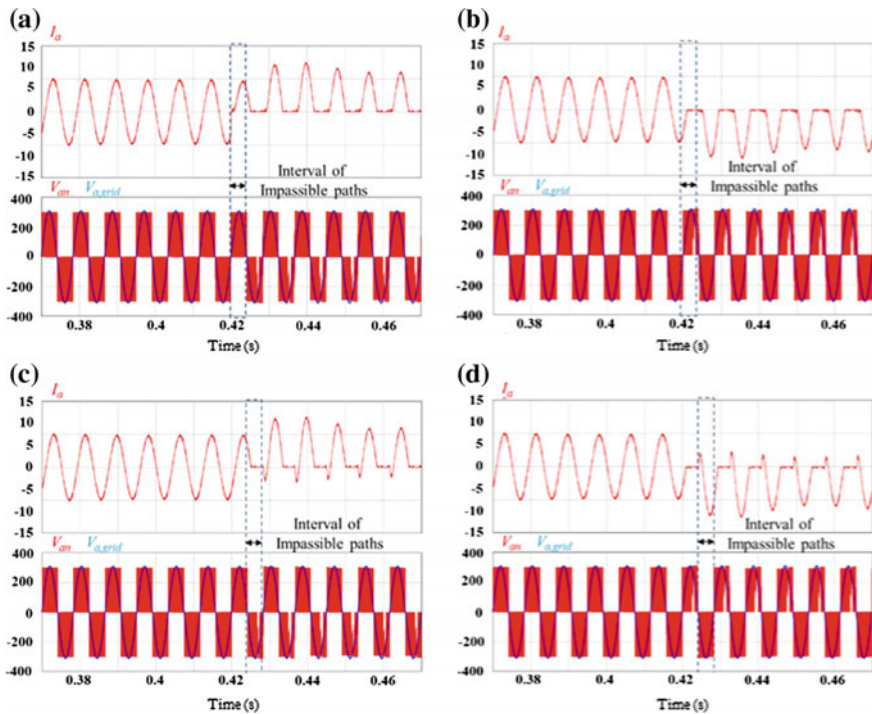


Fig. 2.24 Current distortion and a-phase pole voltage of open-switch faults for a power factor of 0.5: **a** S_{a2} , **b** S_{a1} , **c** S_{a3} , **d** S_{a4} (reprinted from [8], Fig. 8)

C. Experimental results of the switch open-circuit fault detection in NPC three-level rectifiers/inverters

The steps for switch fault detection in NPC three-level rectifiers/inverters is as follows:

- (1) Calculation of the current sign ($C_{pre,sign}$) as shown in Fig. 2.22
- (2) Calculation of the zero range using (2.5) and (2.6)
- (3) If it exceeds only D_{14} , an S_{x1} or S_{x4} open-circuit fault occurs. Then the final position of the open-circuit fault is determined by $C_{pre,sign}$. If it exceeds D_{14} and D_{23} , an S_{x2} or S_{x3} open-circuit fault occurs. Then final position of the open-circuit fault is decided by $C_{pre,sign}$.

Figure 2.26 shows the experimental setup and the simulation and experimental parameters are shown in Table 2.6.

Figure 2.27 shows distorted currents caused by open-switch faults in a rectifier at 600 rpm. The negative current remains zero for some time after the zero crossing point when an S_{a1} open-switch fault occurs, as shown in Fig. 2.27a. An S_{a4} open-switch fault prevents the flow of positive a-phase current for some time after

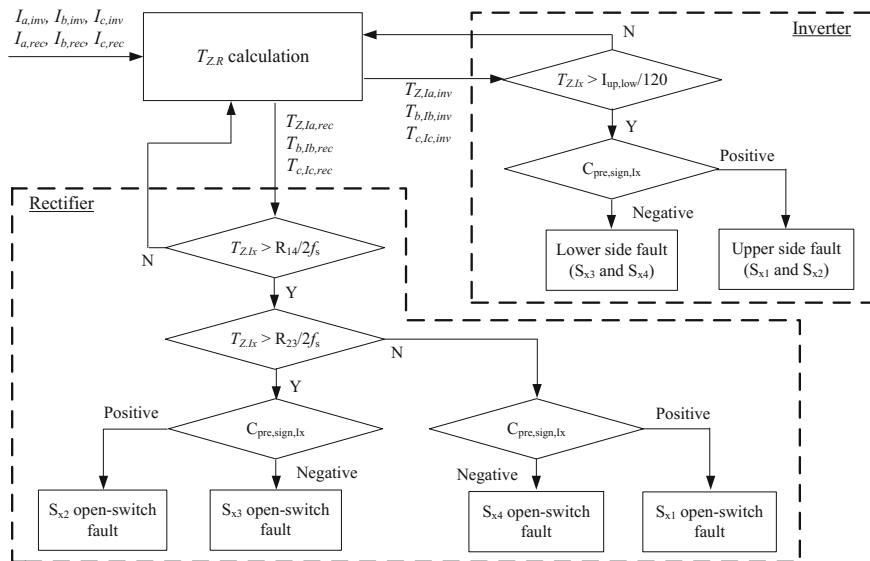


Fig. 2.25 Block diagram of the open-switch fault detection method in a back-to-back converter (reprinted from [8], Fig. 14)

Table 2.6 Simulation and experimental parameters

<i>Generator</i>			
Rated power	11 kW	Rated power	191 Vrms
pole	6	pole	1450 rpm
Stator resistance	0.099 Ω	Stator resistance	4.07/4.65 mH
<i>System parameter</i>			
DC-link voltage	600 V	DC-link voltage	380 Vrms
DC-link capacitance	1100 μF	DC-link capacitance	60 Hz
Switching frequency	10 kHz	Switching frequency	100 μs
<i>Detection parameter</i>			
R_{14}	0.075	$R_{23}/I_{up,low}$	0.3

the zero crossing point, as shown in Fig. 2.27b. The negative current in the a-phase becomes zero when an S_{a2} open-switch fault occurs, as shown in Fig. 2.27c. An S_{a3} open-switch fault prevents the flow of positive current in the a-phase, as shown in Fig. 2.27d. This characteristic of open-switch faults, which is verified by experimental results, is the same as that of the simulated results.

Figure 2.28 shows the performance of the open-switch fault detection method in a rectifier at 600 rpm. $T_{Z,Lx}$ is always smaller than D_{14} for normal operation. However, $T_{Z,Lx}$ increases when the current is zero because of an open-switch fault. Then, an open-switch fault is detected when $T_{Z,Lx}$ exceeds D_x ($x = 14$ and 23). The detection signal, which is indicated by the red line, represents the location of the

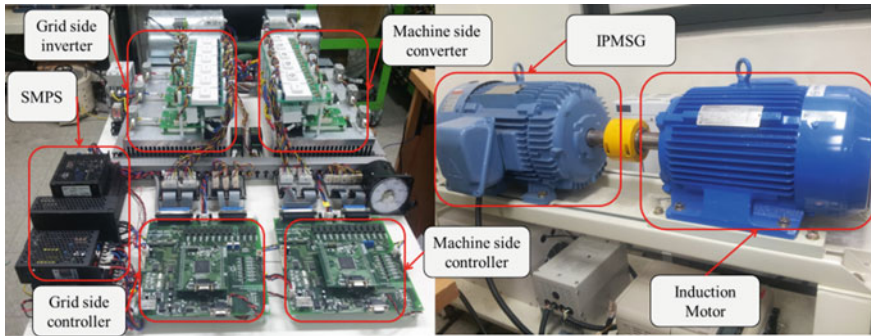


Fig. 2.26 Experimental setup of a back-to-back converter using a NPC three-level topology (reprinted from [8], Fig. 15)

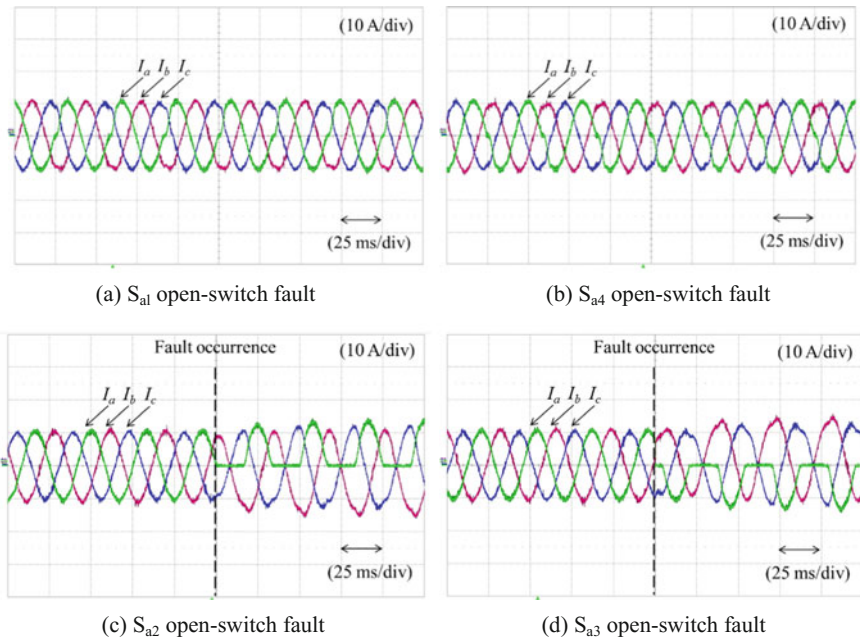


Fig. 2.27 Current distortion caused by open-switch faults in the rectifier of a PMSG at 600 rpm (reprinted from [8], Fig. 16)

open-switch fault. The open-switch fault detection method determines the location of the open-switch fault using T_{ZLx} and the previous sign of the current, as shown in Fig. 2.28. Each fault detection signal is sent within one period of the current. Figure 2.29 shows the performance of the open-switch fault detection method in a rectifier at 1200 rpm. Because an angular frequency of 1200 rpm is twice that of

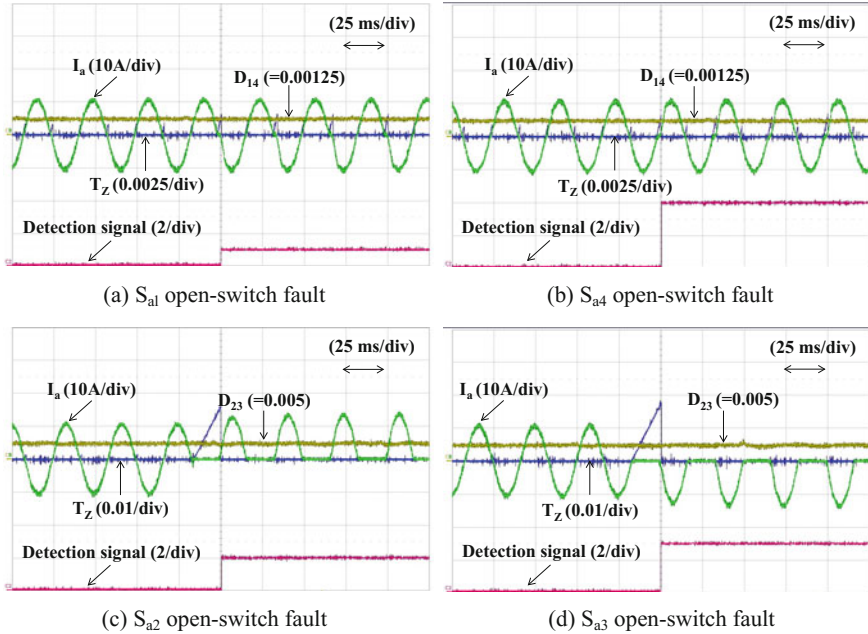


Fig. 2.28 Experimental results for the proposed open-switch fault detection in the rectifier of a PMSG at 600 rpm (reprinted from [8], Fig. 17)

600 rpm, D_{14} and D_{23} , which are calculated using (1) and (2), decrease in magnitude by half, and their values are shown in Fig. 2.29. Similar to the case in Fig. 2.28, $T_{z,ix}$ increases after an open-switch fault occurs, and the location of the open-switch fault is determined within one period of the current.

Figure 2.30 shows the performance of the open-switch fault detection method in an inverter at a unity power factor. In the inverter, S_{x1} and S_{x2} (S_{x3} and S_{x4}) open-switch faults lead to the same current pattern shown in Fig. 2.30. An open-switch fault is detected when $T_{z,ix}$ exceeds $D_{up,low}$. A value of 1 for the red line, which is the detection signal, indicates that there is one S_{x1} and S_{x2} open-switch fault. Meanwhile, a value of 2 for the red line indicates that there is one S_{x3} and S_{x4} open-switch fault. The open-switch fault detection method determines the location of the open-switch fault, as shown in Fig. 2.30. Each fault detection signal is sent within one period of the current.

Figure 2.31 shows the performance of the open-switch fault detection method in an inverter at a power factor of 0.5. In this case, S_{x1} and S_{x2} (S_{x3} and S_{x4}) open-switch faults lead to different current patterns. An S_{x2} (S_{x3}) open-switch fault leads to a zero current for a longer duration than an S_{x1} (S_{x4}) open-switch fault, as shown in Fig. 2.31. Although the power factor is not unity, the open-switch fault detection method accurately determines the location of the open-switch fault. Each fault detection signal is sent within one period of the current.

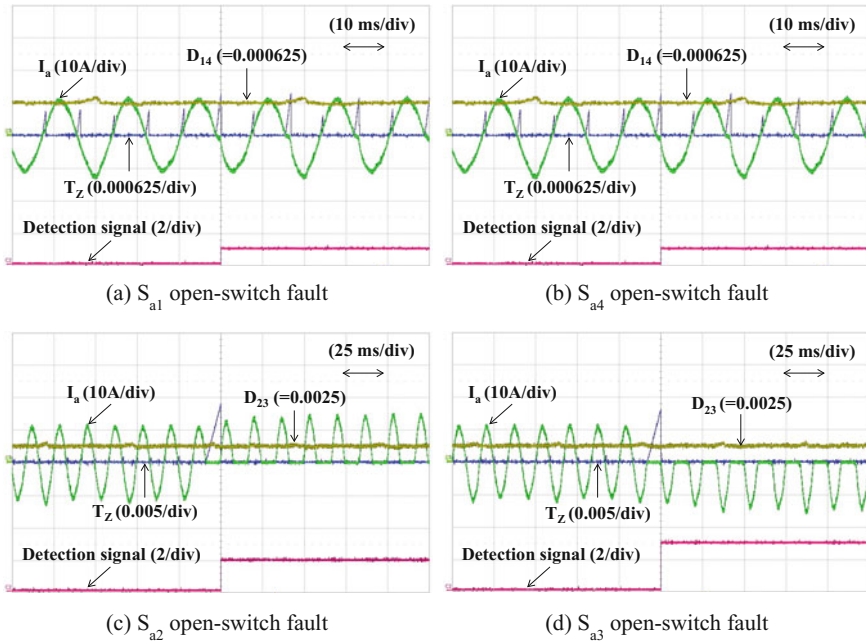


Fig. 2.29 Experimental results for the proposed open-switch fault detection in the rectifier of a PMSG at 1200 rpm (reprinted from [8], Fig. 18)

2.4 Switch Open-Circuit Fault Detection Method for T-Type Three-Level Inverter

There are three switching states for three-level topologies. The first switching state is named P, and this means that S_{x1} and S_{x2} are ON and that S_{x3} and S_{x4} are OFF. The next switching state is named O, and this means that S_{x2} and S_{x3} are ON and that S_{x1} and S_{x4} are OFF. The switching state N means that S_{x1} and S_{x2} are OFF and that S_{x3} and S_{x4} are ON. Depending on the current direction and switching state, there are six current paths in the T-type topology, as shown in Fig. 3.32.

2.4.1 Switch Open-Circuit Fault Detection Method Using Current Distortion

A. The effects on current depending on the position of an open-circuit fault

The current paths of inverter and rectifier operations are different. For inverter operation with a unity power factor, most of the positive current flows through the paths of Fig. 2.32b, c, and most of the negative current flows through the paths of

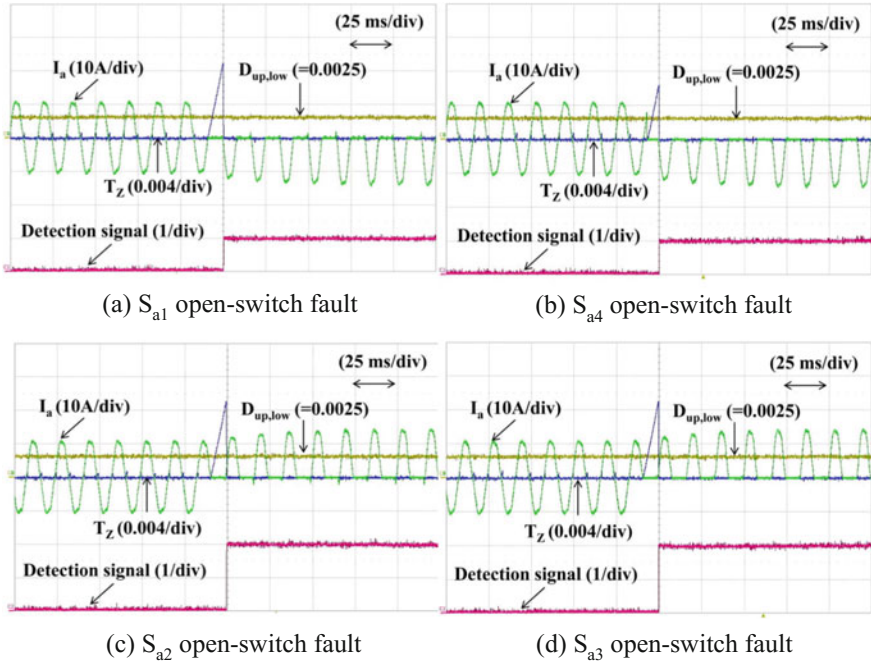


Fig. 2.30 Experimental results for the open-switch fault detection in an inverter at a unity power factor (reprinted from [8], Fig. 19)

Fig. 2.32d, e. Therefore, in a NPC inverter, the P-switching state of Fig. 2.32d is made infeasible by an S_{x1} or S_{x2} open-switch fault regardless of the position of the open-switch fault. This means that NPC inverters have a structural limitation to realizing tolerance control without additional devices. On the other hand, in rectifier operation with a unity power factor, most of the positive current flows through the paths of Fig. 2.32a, b, and most of the negative current flows through the paths of Fig. 2.32e, f. These paths do not include the current flowing through S_{x1} and S_{x4} .

- S_{x1} open-circuit faults

In T-type three-level inverters, S_{x1} open-circuit fault makes the P-switching state infeasible. This means that the current path of Fig. 2.32d cannot be generated. If R-L load is connected to the output of the inverter, an S_{x1} open-circuit fault leads to variations of the load voltage, and an undesired current flows through the O-switching state instead of the P-switching state. However, the grid voltage and back EMF of the motor drive do not generate any current due to the impossibility of the P-switching state.

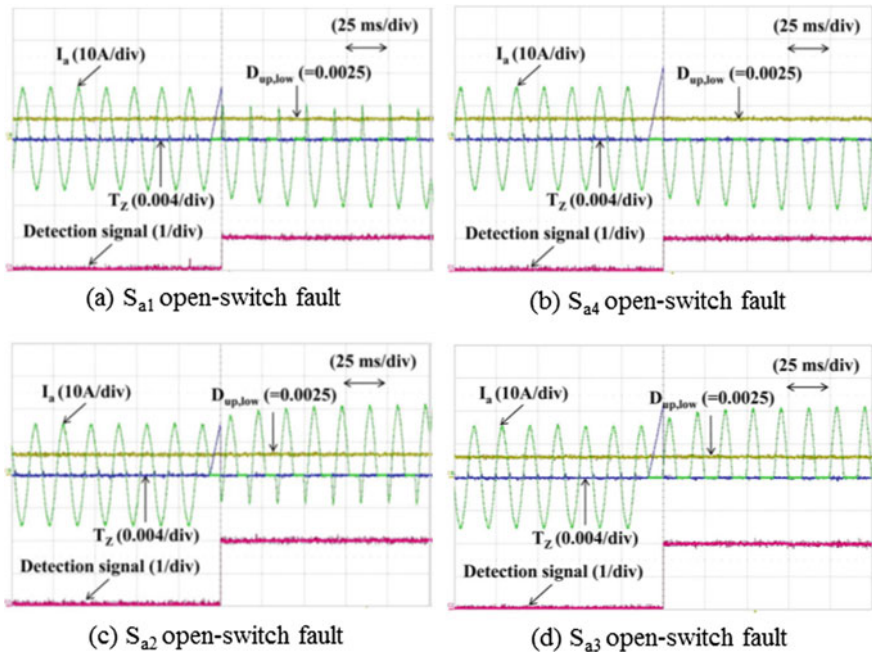


Fig. 2.31 Experimental results for the open-switch fault detection in an inverter at a power factor of 0.5 (reprinted from [8], Fig. 20)

- S_{x2} open-circuit faults

In T-type three-level inverters, an S_{x2} open-circuit fault influences the O-switching state. Therefore, the current path of Fig. 2.32e cannot be generated.

- S_{x3} open-circuit faults

In T-type three-level inverters, an S_{x3} open-circuit fault influences the O-switching state. This is related to the current path of Fig. 2.32b which cannot be generated.

- S_{x4} open-circuit fault

S_{x4} open-circuit faults lead to the impossibility of the N switching state. As a result, the current path of Fig. 2.32c cannot be generated. Similar to S_{x1} open-circuit faults, in the R-L load condition, current is generated by the feasible O-switching state. On the other hand, there is no current in grid-connected and motor drive applications when an S_{x4} open-circuit fault occurs regardless of the validity of the O-switching state.

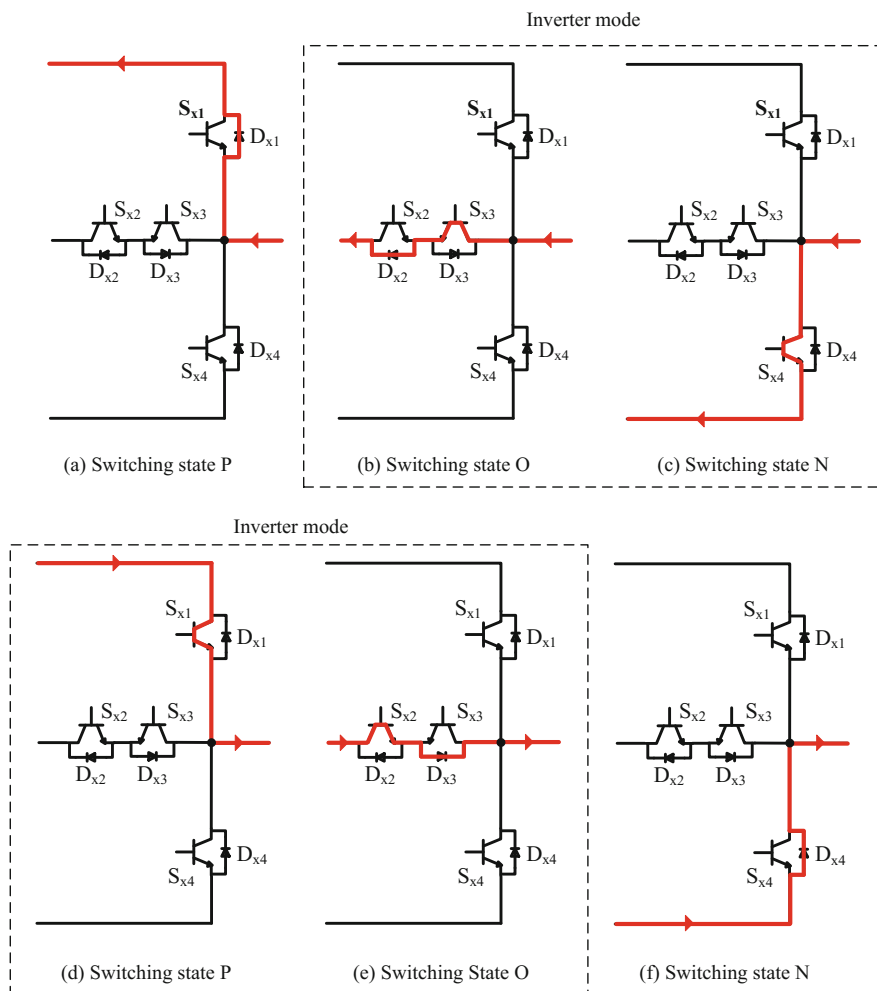


Fig. 2.32 Current paths depending on the current direction and operating state

The feasible and infeasible switching states of T-type three-level converter depending on the position of the open-switch fault are summarized in Table 2.7.

B. Switch open-circuit fault detection method for T-type converters [6]

- The classification of upper switch (S_{x1} , S_{x2}) and lower switch (S_{x3} , S_{x4}) open-circuit faults

Under normal conditions, the average of the phase current is zero. However, in faulty cases, the value of the phase current's average is changed. If an open-switch fault occurs in S_{x1} or S_{x2} , the average of the phase current is a negative value because the positive phase current is distorted as shown in Fig. 2.33. If an

Table 2.7 Feasible and infeasible switching states of a T-type three-level converter depending on the position of an open-switch fault

Position of open-switch fault	Feasible switching state	Infeasible switching state
S_{x1}	N (Fig. 2.32c, f) O (Fig. 2.32b, e) P (Fig. 2.32a)	P (Fig. 2.32d)
S_{x2}	N (Fig. 2.32c, f) O (Fig. 2.32b) P (Fig. 2.32a, d)	O (Fig. 2.32e)
S_{x3}	N (Fig. 2.32c, f) O (Fig. 2.32e) P (Fig. 2.32a, d)	O (Fig. 2.32b)
S_{x4}	N (Fig. 2.32f) O (Fig. 2.32b, e) P (Fig. 2.32a, d)	N (Fig. 2.32c)

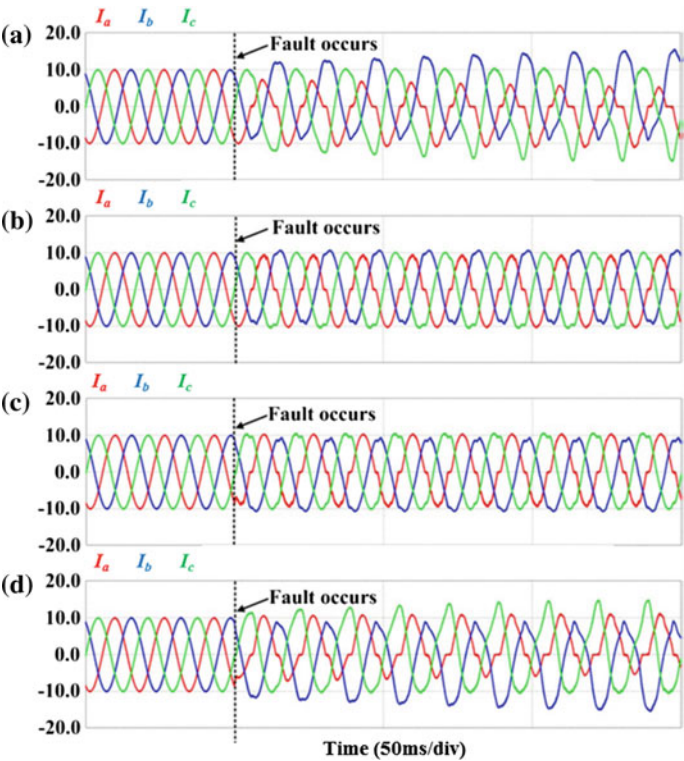


Fig. 2.33 Phase current in a T-type three-level inverter with RL load depending on the position of an open-circuit fault: **a** S_{x1} , **b** S_{x2} , **c** S_{x3} , **d** S_{x4} (reprinted from [6], Figs. 6–9)

open-switch fault occurs in S_{x3} or S_{x4} , the average of the phase current has a positive value because the negative phase current is distorted in the faulty leg.

The averages of the other phase currents are also changed due to distortions of the phase current in the faulty leg. However, if these values are used directly, they may lead to a false alarm when harmonic components exist in the phase current or when this system is notably under fast transients. To improve the accuracy of detection, the normalized current method is employed. The normalized current can be obtained by the following equation:

$$\begin{aligned} I_s &= \sqrt{I_{qs}^2 + I_{ds}^2} \\ I_{xN} &= \frac{I_x}{I_s} \end{aligned} \quad (2.13)$$

where $x = a, b, c$, and I_{ds} and I_{qs} are the reactive and active currents in the stationary reference frame, respectively.

The average of the phase current ($I_{xN,avg}$) for one-fundamental period can be expressed as:

$$I_{xN,avg} = \int_0^{2\pi} I_{xN} \quad (2.14)$$

Using these values, it is possible to identify the faulty leg and whether the open-switch faults occur in one of the two switches S_{x1} and S_{x2} or in one of the two switches S_{x3} and S_{x4} . To improve accuracy, the threshold value I_{thr} is set. It is summarized as:

$$\begin{aligned} I_{xN,avg} > I_{thr} &: & U_x &= 1 \\ I_{xN,avg} < -I_{thr} &: & U_x &= -1 \\ -I_{thr} < I_{xN,avg} < I_{thr} &: & U_x &= 0 \end{aligned} \quad (2.15)$$

- An analysis of the characteristic difference between upper switch (S_{x1} , S_{x2}) and lower switch (S_{x3} , S_{x4}) open-circuit faults

As mentioned above, by using the average phase current ($I_{xN,avg}$), it is possible to divide faults into upper switch (S_{x1} , S_{x2}) and lower switch (S_{x3} , S_{x4}) open-circuit faults. However, the positions should be classified as S_{x1} and S_{x2} (S_{x3} and S_{x4}) in detail.

To do this, it is necessary to analyze T-type three-level converter operation in the case of a switch fault. The operation conditions can be divided into the R-L load condition and the voltage condition. The T-type three-level converter operates as an inverter, and the P-switching state, which is a valid switching state, leads to the current flow. In the case of the RL load condition, when the P-switching state is infeasible, current flows through S_{x2} as shown in Fig. 2.34. This circuit is the same as that of the O-switching state. Although the O-switching state is not a valid

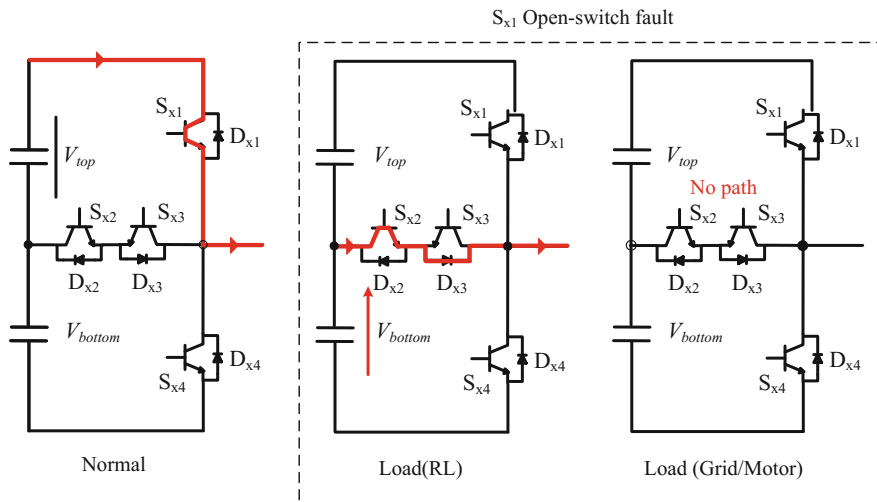


Fig. 2.34 Current path of a T-type three-level converter with an S_{x1} open-circuit fault during the P switching state

switching state, current flows because the current is determined by the output voltage in the R-L load condition. However, in the case of the grid-connected condition or the motor drive condition, since the current is affected by both the output voltage and the grid voltage or the back EMF of the motor, current does not flow if the P-switching state is infeasible as shown in Fig. 2.34.

In addition, two DC-link voltages are changed owing to the current variation of an S_{x1} open-circuit fault as shown in Fig. 2.34. The P-switching state transfers power from two DC-link capacitors to the output under normal operation. However, an S_{x1} open-circuit fault in the R-L load condition leads the current flow through the neutral-point and it flows from the bottom capacitor. This means that S_{x1} open-circuit faults cause different voltage variations in both of the DC-link capacitors.

S_{x2} open-circuit faults make the O-switching state infeasible which is not a valid switching state. Therefore, it generates current directly and just operates as a freewheeling path for the current. The current generated by a valid switching state flows continuously through D_{x4} when an S_{x2} open-circuit fault occurs. S_{x2} open-circuit faults makes the same current flow, as shown in Fig. 2.35, regardless of the condition of the load (R-L or voltage). DC-link voltage variation is also generated by S_{x2} open-circuit faults. The current flows through the neutral-point and it flows to the bottom capacitor which is the opposite situation when compared to S_{x1} open-circuit faults.

Using the change of the two capacitor voltages, a faulty switch can be identified between switch S_{x1} and switch S_{x2} or between switch S_{x3} and switch S_{x4} . If V_{dc1} is bigger than V_{dc2} , the open-switch fault occurs in switch S_{x1} or switch S_{x3} . Reversely, if V_{dc2} is larger than V_{dc1} , the open-switch fault occurs in switch S_{x2} or switch S_{x4} .

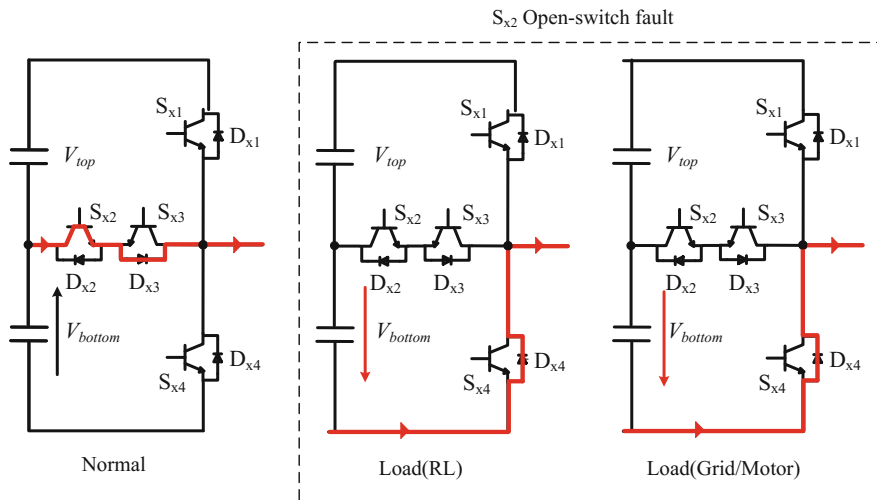


Fig. 2.35 Current path of a T-type three-level converter with an S_{x2} open-circuit fault during the O switching state

To improve accuracy, the threshold value V_{thr} is set. It is expressed as:

$$\begin{aligned}
 V_{top} - V_{bottom} > V_{thr} : & \quad V_x = 1 \\
 V_{top} - V_{bottom} < -V_{thr} : & \quad V_x = -1 \\
 -V_{thr} < V_{top} - V_{bottom} < V_{thr} : & \quad V_x = 0
 \end{aligned} \quad (2.16)$$

C. Experimental results of switch open-circuit fault detection in T-type three-level inverters

The steps for the fault diagnosis of T-type three-level inverters is as follows.

- (1) Calculate the average of the normalized phase currents.
- (2) Using these values, identify the faulty leg and whether the open-switch faults occur in one of the two switches S_{x1} and S_{x2} or in one of the two switches S_{x3} and S_{x4} .
- (3) Identify the location of the faulty switch between S_{x1} and S_{x2} or between S_{x3} and S_{x4} using the change of the two capacitor voltages. Values of the diagnostics variables are shown in Table 2.9.

Figure 2.36 shows experimental results of the proposed fault diagnosis method under the parameters of Table 2.8 when an open-switch fault occurs in switches S_{a1} ,

Table 2.8 Experimental parameters

DC-link voltage	200 V	Fundamental frequency	60 Hz
Control period	100 μ s	Load	10 mH, 10 Ω
Switching period	10 kHz	I_{thr} , V_{thr}	0.08, 10 V

Table 2.9 Values of the diagnostics variables

Fault position	Diagnosis variables			
	U_a	U_b	U_c	V_x
S_{a1}	-1	+1	-	+1
S_{a2}	-1	+1	-	-1
S_{a3}	+1	-1	-	+1
S_{a4}	+1	-1	-	-1
S_{b1}	-	-1	+1	+1
S_{b2}	-	-1	+1	-1
S_{b3}	-	+1	-1	+1
S_{b4}	-	+1	-1	-1
S_{c1}	+1	-	-1	+1
S_{c2}	+1	-	-1	-1
S_{c3}	-1	-	+1	+1
S_{c4}	-1	-	+1	-1

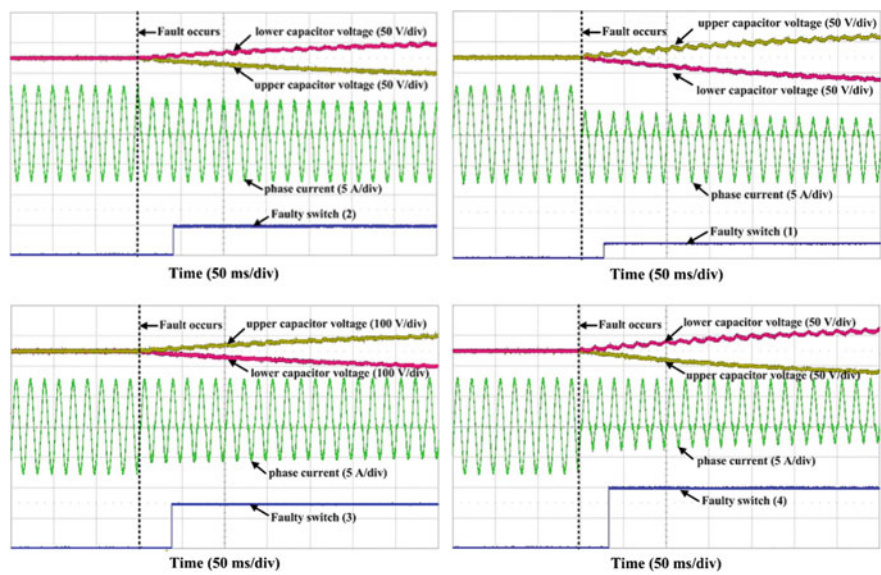


Fig. 2.36 Experiment results of the proposed fault diagnosis method (reprinted from [6], Figs. 26–29)

S_{a2} , S_{a3} , and S_{a4} , respectively. After the fault, the phase current is distorted, and the upper capacitor voltage becomes larger than the lower capacitor voltage as discussed in the previous analysis. The faulty switch is detected within 30 ms. In all of the cases, the faulty switch is identified accurately in about 50 ms. More time is needed to detect the fault switch when an open-switch fault occurs in neutral-point

switches (S_{x2} or S_{x3}) than when an open-switch fault occurs in half-bridge switches (S_{x1} or S_{x4}). This is because the phase currents are less distorted in the neutral-switch fault case than those of the half-bridge switch fault case. This diagnosis time is closely related to the magnitude of the phase current, the size of the capacitor, and the threshold value. Experimental results show that the proposed fault diagnosis method precisely detects the faulty switch.

2.5 Switch Open-Circuit Fault Detection Method for T-Type Three-Level Rectifiers

2.5.1 Switch Open-Circuit Fault Detection Method Using Current Distortion

A. Analysis of T-type rectifiers in the presence of an open-switch fault.

Depending on the operating state and current direction, there are six paths as shown in Fig. 2.37. In the rectifier, almost all of the current is generated when the operating state is O, and the current continuously flows through a diode if the operating state is changed to P or N. This means that the infeasibility of the O-operating state leads to the zero current regardless of the P-operating state.

There are three paths when the current is positive. In the positive current part, most of the current of the rectifier which has a unity power factor, flows through paths (a) and (b). Therefore, the range of a-path (c) is small compared to ranges of paths (a) and (b). Hence, an S_{x3} open-switch fault in the O-operating state is fatal to rectifier operation and causes current distortion. On the other hand, an S_{x1} open-switch fault does not cause current distortion in the P-operating state because the current flows through a diode. In the N-operating state, the current flows through S_{x4} . An S_{x4} open-switch fault has little effect on the current when the rectifier is operated with a unity power factor. In addition, S_{x1} also does not affect the current in the negative current part.

B. Current distortion of T-type three-level rectifiers in the grid-connected condition [7]

Figure 2.38a shows the current, DC-link voltage, and pole voltage when an S_{a2} open-switch fault occurs. The S_{a2} open-switch fault has a fatal effect on the input current. In the negative current part, the valid O-operating state, which is shown in Fig. 2.37e, becomes impossible. Therefore, the whole negative current cannot be generated. Moreover, the DC-link voltage is largely changed. The negative current of Fig. 2.38a is caused by the decreased DC-link voltage. When the DC-link voltage is lower than the line-to-line peak voltage of the grid, the current can flow into the DC-link capacitor from the grid through the diodes of the rectifier.

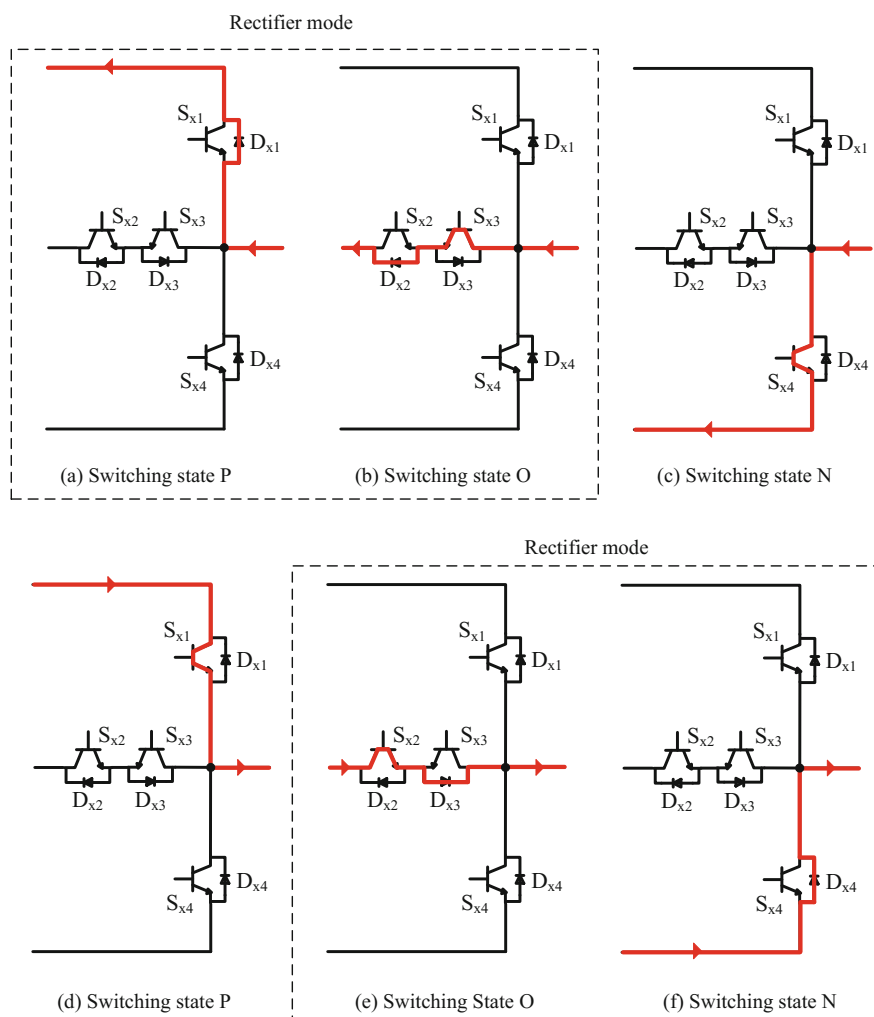


Fig. 2.37 Current paths depending on the current direction and operating state

Although the P-operating state is possible, current does not flow because P is not a valid operating state. The pole voltage of Fig. 2.38a does not have meaning in the negative current part. This is because, when the input voltage is a valid operating state O, the rectifier inner circuit can be an open circuit by an S_{a2} open-switch fault Fig. 2.40.

Figure 2.38b shows the current, DC-link voltage and pole voltage when an S_{a3} open-switch fault occurs. Like an S_{a2} open-switch fault, a valid operating state is impossible. Therefore, an S_{a3} open-switch fault makes the positive current zero for some parts and causes DC-link voltage ripple. Open-switch faults of S_{a2} and S_{a3} in

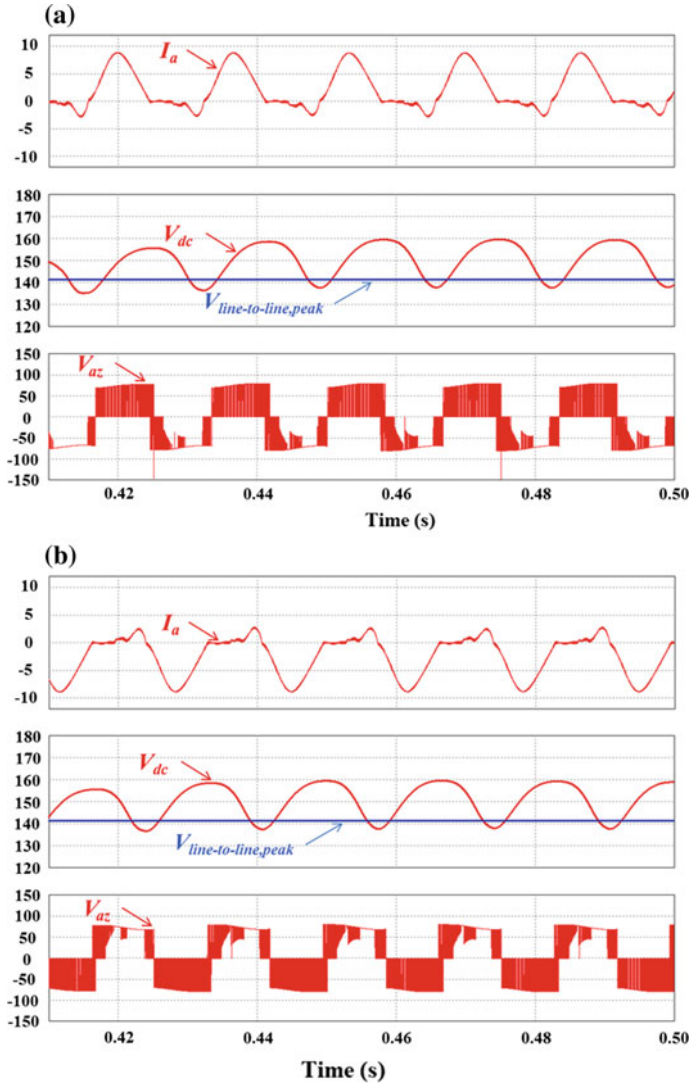


Fig. 2.38 Rectifier waveforms: I_a , V_{dc} , $V_{line-to-line,peak}$, and V_{az} : **a** S_{x2} , **b** S_{x3} (reprinted from [7], Figs. 5, 6)

the b-phase and c-phase legs cause the same current distortion as those of the a-phase leg.

To detect all of the open-switch faults without additional devices, current shapes should be considered. The input current angle is the same as the grid voltage angle with a unity power factor. Therefore, the grid voltage angle is used to detect open-switch faults.

By using the measured grid voltages, the d-axis and q-axis voltages are calculated as:

$$\begin{aligned} E_{ds} &= \frac{2E_a - E_b - E_c}{3} \\ E_{qs} &= \frac{E_b + E_c}{\sqrt{3}} \end{aligned} \quad (2.17)$$

By using the d-axis and q-axis voltages, the grid voltage angle is calculated as:

$$\theta = \tan^{-1} \left(\frac{E_{qs}}{E_{ds}} \right) \quad (2.18)$$

A calculated angle (θ) of (2.18) is more accurate than the angle from the grid current because the grid voltage always has a large value. Depending on an position of the open-switch fault, the angle value which makes the current zero is different. Figure 2.39 shows the angle range with zero current depending on the position of an open-switch fault. The zero current range is changed by the DC-link capacitor and load current. A large DC-link capacitor decreases the DC-link voltage change and keeps the DC-link voltage higher than the grid rectifier voltage for a long time. This means that the zero current range is expanded. On the other hand, a small DC-link capacitor reduces the zero current range. A large load current also reduces the zero current range because a large current flows of the load from the DC-link capacitor. However, the start angle value of the zero current range is always the same regardless of the DC-link capacitor value and load current. When an S_{a2} open-switch fault occurs, zero current is generated from the angle value $\pi/2$. In an S_{a3} open-switch fault, the current becomes zero from the angle value $3\pi/2$.

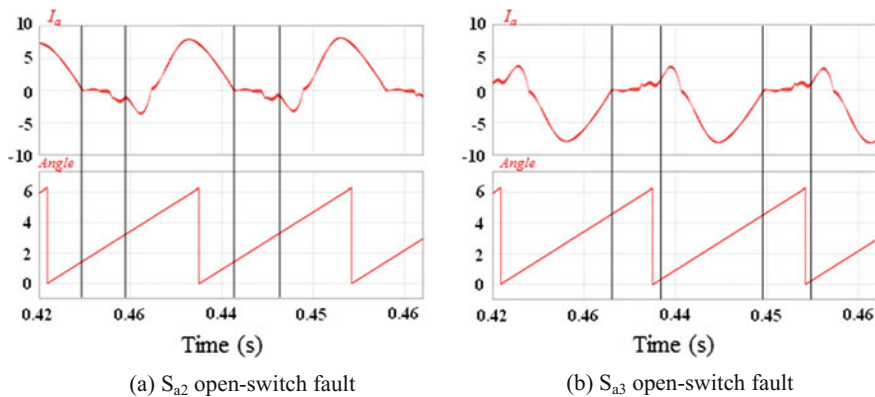


Fig. 2.39 Angle value with zero current according to the position of an open-switch fault in the a-phase leg (reprinted from [7], Fig. 7)

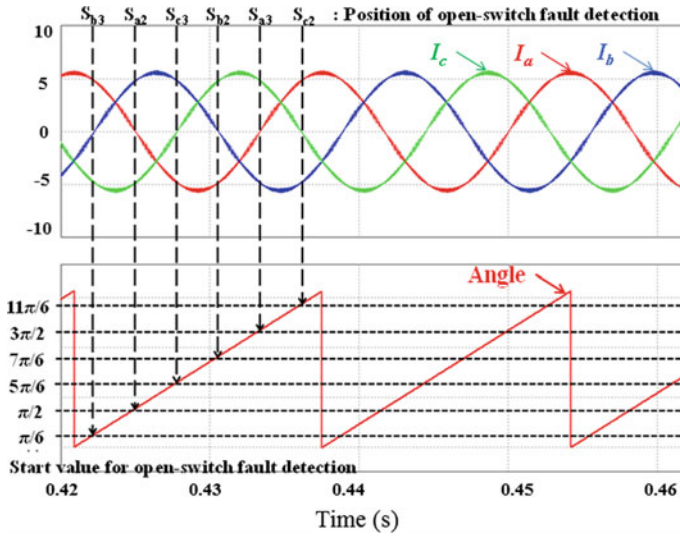


Fig. 2.40 Detection angle values according to the position of an open-switch fault in all of the phases (reprinted from [7], Fig. 8)

Through considerations of b-phase and c-phase current distortions, the start angle values which lead to zero current are defined as shown in Fig. 2.40. To detect the position of an open-switch fault, the angle value and differential equation for each of the currents are used, and the differential equation is defined as:

$$\Delta I = \frac{dI_x}{dt} = \frac{I_x[n] - I_x[n-1]}{T_{fault}}, \quad \begin{cases} x = a, & \theta = \pi/2 \sim 2\pi/3, 3\pi/2 \sim 5\pi/3 \\ x = b, & \theta = \pi/6 \sim \pi/2, 7\pi/6 \sim 4\pi/3 \\ x = c, & \theta = 5\pi/6 \sim \pi, 11\pi/6 \sim 2\pi \end{cases} \quad (2.19)$$

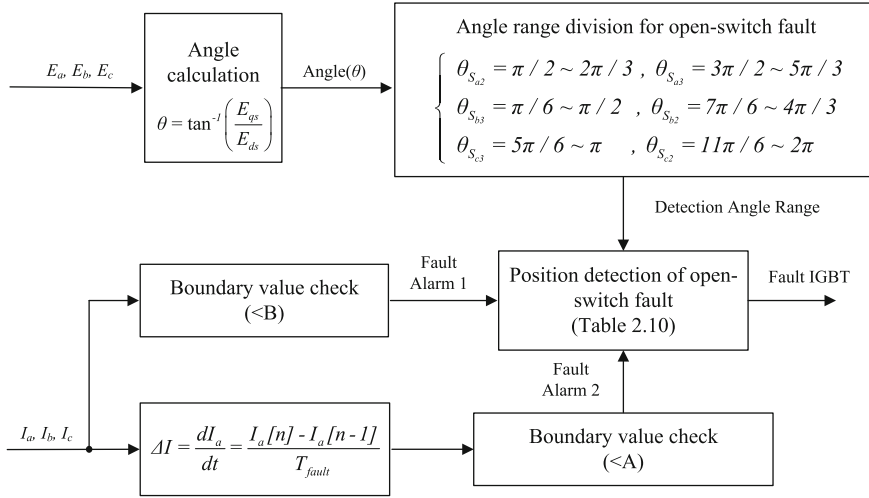
where T_{fault} is a period of the differential equation and I_x ($x = a, b, c$) is the measured current. The proposed detection method monitors open-switch faults for the $\pi/6$ range from each start angle value.

The derivative value of the current at the detection angle range becomes zero when an open-switch fault occurs because the slope of the current is steepest at the zero crossing point of the current. The derivative value of the current has its largest value at the zero crossing point of the normal current. Therefore, if an open-switch fault occurs, a dramatic change can be observed because the current and the derivative value of the current become zero at the zero crossing point of the current.

Consequently, the proposed open-switch detection method uses the current value and grid angle as shown in Table 2.10. Moreover, a block diagram of the summarized open-switch fault detection method is shown in Fig. 2.41. For the final decision determination of an open-switch fault, both of the fault alarms 1 and 2 have to be generated, which means that the input current has a smaller value than

Table 2.10 Open-switch fault detection table

Detection angle range	$\pi/6 \sim \pi/3$	$\pi/2 \sim 2\pi/3$	$5\pi/6 \sim \pi$	$7\pi/6 \sim 4\pi/3$	$3\pi/2 \sim 5\pi/3$	$11\pi/6 \sim 2\pi$
Detection boundary value	$ I_b < A$, $ dI_b/dt < B$	$ I_a < A$, $ dI_a/dt < B$	$ I_c < A$, $ dI_c/dt < B$	$ I_b < A$, $ dI_b/dt < B$	$ I_a < A$, $ dI_a/dt < B$	$ I_c < A$, $ dI_c/dt < B$
Detection switch	S_{b3}	S_{a2}	S_{c3}	S_{b2}	S_{a3}	S_{c2}

**Fig. 2.41** Block diagram of the proposed detection method for a T-type rectifier (reprinted from [7], Fig. 9)

the boundary value (0.2), and the derivative value of the current is smaller than the boundary value (0.5).

In the discussed open-switch fault detection method, the boundary values of the current and the differential equation of the current are important factors in the performance of the open-switch fault detection. Ideally, an open-switch fault causes the result of (2.19) to be 0 for some part of the current. Therefore, an open-switch fault can be detected when the result of (2.19) is 0. In such a case, the boundary values can be chosen as 0. However, boundary values should be used, excluding 0, because currents contain ripple and noise components. Selecting boundary values

Table 2.11 Simulation and experimental results

DC-link voltage	150 V	Grid line-to-line voltage	150 Vrms
DC-link capacitor	550 μ F	Grid frequency	60 Hz
Switching frequency	10 kHz	Load	33.3 Ω
Control period	100 μ s	A, B	0.5, 0.2

for currents should consider the current ripple, and this value should be larger than the current ripple. However, a very large boundary.

C. Experimental results of switch open-circuit fault detection in T-type three-level rectifiers

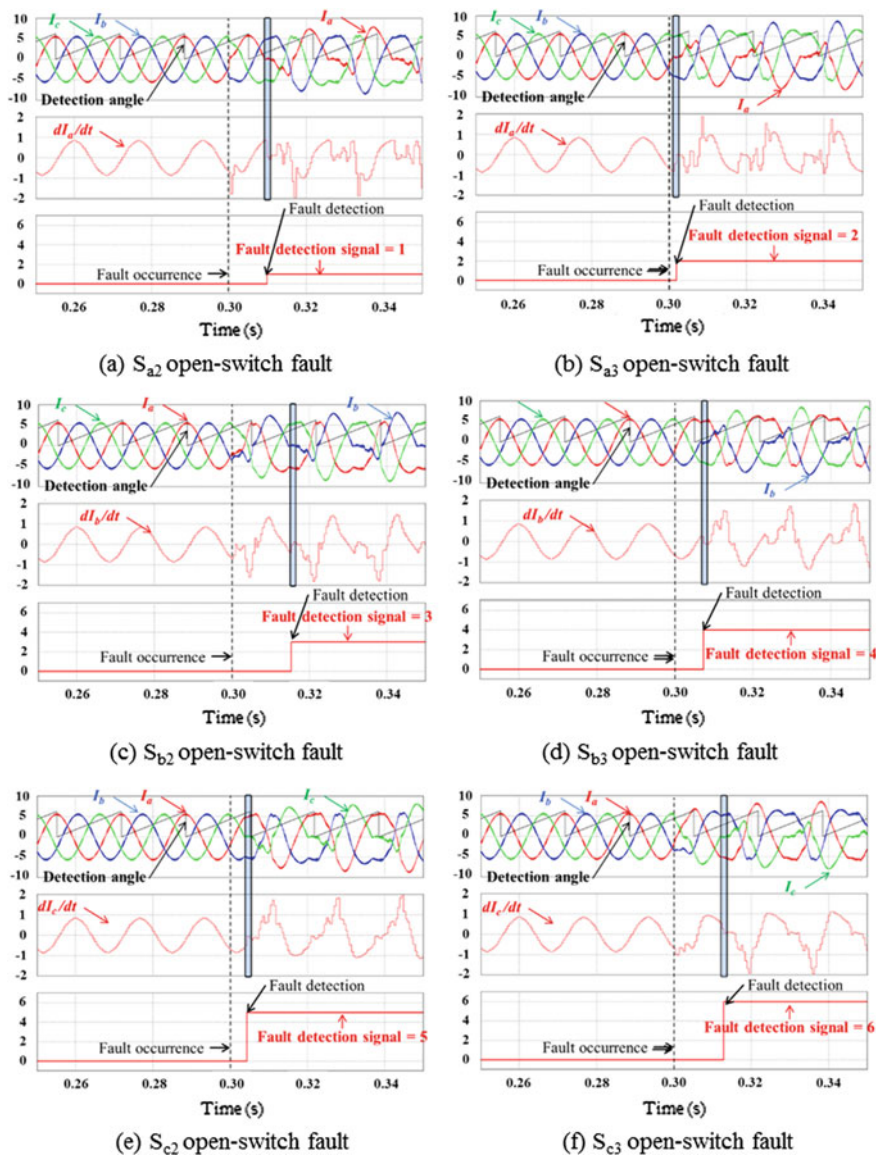


Fig. 2.42 Currents and fault detection signal depending on the open-switch fault position (reprinted from [7], Fig. 16)

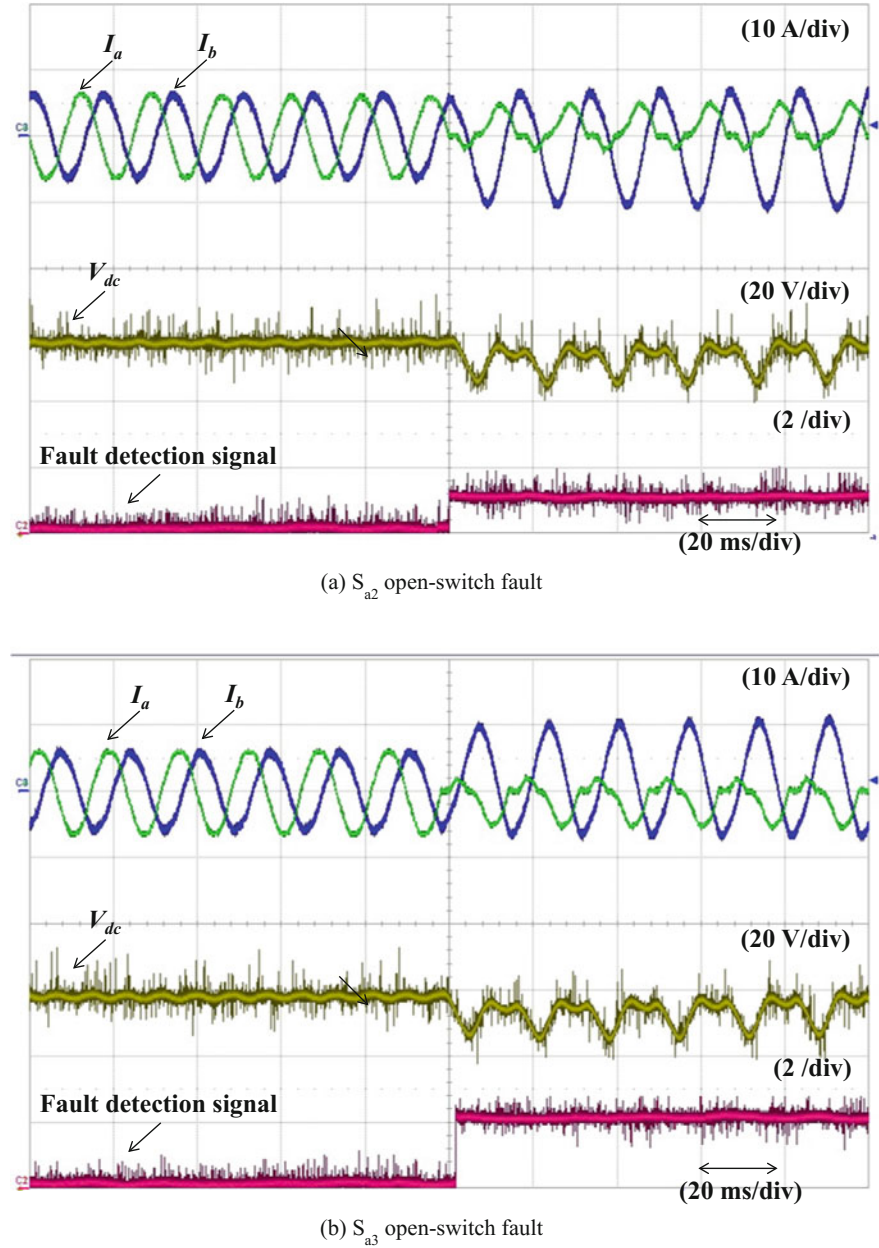


Fig. 2.43 Experimental results of open-switch fault detection (reprinted from [7], Fig. 21)

The steps for the fault diagnosis of T-type three-level rectifiers

- (1) Calculate the grid angle using (2.18).
- (2) During 60° from the six points shown in Fig. 2.40, calculate (2.19).
- (3) Determine the position of the switch open-circuit fault with Table 2.10.

The simulation and experiment was implemented under the parameter of Table 2.11.

Figure 2.42 shows the input currents, fault detection angle, fault detection signal, and derivation of the current flowing through a leg that contains a fault switch. The open-switch fault occurs at 0.4 s, and the fault detection signal has a value of 1, 2, 3, 4, 5, and 6 depending on the position of the open-switch fault. The fault detection signal is generated by the rule of Table 2.10. In Fig. 2.42a, the fault detection signal becomes 1 when the a-phase current and the derivation of this current go into the boundary value at the detection angle $\pi/2$ of Table 2.10. The figures shown in Fig. 2.42b–f, also show the open-switch fault detection process. An open-switch fault of all the switches is detected in a period of the grid frequency (60 Hz) regardless of the position of the open-switch fault.

Figure 2.43a, b show the input currents (I_a and I_b), DC-link voltage, and fault detection signal when S_{a2} and S_{a3} open-switch faults occur. The a-phase input current I_a becomes zero at some part of the negative current due to the S_{a2} open-switch fault in Fig. 2.43. When an S_{a3} open-switch fault occurs, the a-phase input current I_a in some part of the positive current becomes zero. The DC-link voltage has a ripple, as shown in Fig. 2.43a, b, and this value is 16 V. The open-switch fault detection method identifies the open-switch fault and the position of the fault switch. The fault detection signal becomes 1, which means that the open-switch fault position is S_{a2} . The fault detection signal becomes 2 after an S_{a3} open-switch fault occurs as shown in Fig. 2.43b. These results are the same as those obtained in simulations.

References

1. Ribeiro, R.L.A., C.B. Jacobina, E.R.C. Silva, and A.M.N. Lima. 2003. Fault detection of open-switch damage in voltage-fed PWM motor drive systems. *IEEE Transaction on Power Electronics* 18 (2): 587–593.
2. Ribeiro, R.L.A., C.B. Jacobina, E.R.C. Silva, and A.M.N. Lima. 2004. Fault-tolerant voltage-fed PWM inverter AC motor drive systems. *IEEE Transaction on Industrial Electronics* 51 (2): 439–446.
3. Kim, T.J., W.C. Lee, and D.S. Hyun. 2009. Detection method for open-circuit fault in neutral-point-clamped inverter systems. *IEEE Transaction on Industrial Electronics* 56 (7): 2754–2763.
4. Choi, U.M., H.G. Jeong, K.B. Lee, and F. Blaabjerg. 2012. Method for detecting an open-switch fault in a grid-connected npc inverter system. *IEEE Transaction on Power Electronics* 27 (6): 2726–2739.

5. Ko, Y.J., K.B. Lee, D.C. Lee, and J.M. Kim. 2012. Fault diagnosis of three-parallel voltage-source converter for a high-power wind turbine. *IET Power Electronics* 5 (7): 1058–1067.
6. Choi, U.M., K.B. Lee, and F. Blaabjerg. 2014. Diagnosis and tolerant strategy of an open-switch fault for T-type three-level inverter systems. *IEEE Transactions on Industry Applications* 50 (1): 495–508.
7. Lee, J.S., and K.B. Lee. 2014. An open-switch fault detection method and tolerance controls based on SVM in a grid-connected T-type rectifier with unity power factor. *IEEE Transactions on Industrial Electronics* 61 (12): 7092–7104.
8. Lee, J.S., K.B. Lee., and F. Blaabjerg. 2015. Open-switch fault detection method of a back-to-back converter using NPC topology for wind turbine systems. *IEEE Transaction on Industrial Electronics* 51 (1): 325–335.
9. Choi, U.M., F. Blaabjerg, and K.B. Lee. 2015. Reliability improvement of a T-type three-level inverter with fault-tolerant control strategy. *IEEE Transaction on Power Electronics* 30 (5): 2660–2673.
10. Choi, U.M., F. Blaabjerg, and K.B. Lee. 2015. Study and handling methods of power IGBT module failures in power electronic converter systems. *IEEE Transaction on Power Electronics* 30 (5): 2517–2533.
11. Choi, U.M., J.S. Lee, F. Blaabjerg, and K.B. Lee. 2016. Open-circuit fault diagnosis and fault-tolerant control for a grid-connected NPC inverter. *IEEE Transactions on Power Electronics* 31 (10): 7234–7247.
12. Lee, J.S., and K.B. Lee. 2015. Open-switch fault tolerance control for a three-level NPC/T-type rectifier in wind turbine systems. *IEEE Transactions on Industrial Electronics* 62 (2): 1012–1021.

Reliability Improvement Technology for Power
Converters

Lee, K.-B.; Lee, J.-S.

2017, IX, 251 p. 210 illus., 147 illus. in color., Hardcover

ISBN: 978-981-10-4991-0